REGULATORY ELEMENTS OF *DROSOPHILA* NON-MUSCLE MYOSIN II

by

RYAN LYNN FREI

A DISSERTATION

Presented to the Department of Chemistry
and the Graduate School of the University of Oregon
in partial fulfillment of the requirements
for the degree of
Doctor of Philosophy

December 2012

DISSERTATION APPROVAL PAGE

Student: Ryan Lynn Frei

Title: Regulatory Elements of *Drosophila* Non-Muscle Myosin II

This dissertation has been accepted and approved in partial fulfillment of the requirements for the Doctor of Philosophy degree in the Department of Chemistry by:

Tom Stevens	Chairperson
Kenneth Prehoda	Advisor
Karen Guillemin	Member
Brad Nolen	Member
Bruce Bowerman	Outside Member

and

Kimberly Andrews Espy	Vice President for Research and Innovation Dean of the Graduate School

Original approval signatures are on file with the University of Oregon Graduate School.

Degree awarded December 2012

DISSERTATION ABSTRACT

Ryan Lynn Frei

Doctor of Philosophy

Department of Chemistry

December 2012

Title: Regulatory Elements of *Drosophila* Non-Muscle Myosin II

Non-muscle myosin II (NM-II) is present in every cell type and moves actin filaments to provide contraction within the cell. NM-II has a motor domain, a neck domain that binds two light chains, a long coiled-coil tail domain, and a carboxyl-terminal tailpiece. NM-II forms bipolar filaments by associating near the carboxyl-terminus of the tail. It has long been known that both the formation of bipolar filaments and enzymatic activity of the motor domain are regulated by phosphorylation of one of the neck-binding light chains, known as the regulatory light chain (RLC). This phosphorylation causes a large-scale conformational shift of both the motor domains and the tail domain. However, the mechanism of this regulation and the elements that mediate the autoinhibition remain unknown.

We have taken a deletional approach to finding the elements necessary for autoinhibition and regulation of filament assembly. We have used salt-dependent pelleting assays, cell culture, and analytical ultracentrifugation to identify two small regions in the IQ motifs of the neck and the carboxyl-terminal tailpiece that are essential for autoinhibition.

Another necessary element for autoinhibition is the fold the coiled coil of

the tail back on itself by means of hinge domains. We used internal deletions, pelleting assays, and thermal stability assays to identify and characterize the flexible hinge domains within the coiled-coil tail of NM-II. These hinges consist of low-stability regions of coiled coil and can be stiffened by introducing mutations that cause the sequence to mimic a more ideal coiled coil. By defining these essential elements of autoinhibition, this work paves the way for a mechanistic understanding of the complex regulation of NM-II in the cell.

This dissertation contains unpublished co-authored material.

CURRICULUM VITAE

NAME OF AUTHOR: Ryan Lynn Frei

GRADUATE AND UNDERGRADUATE SCHOOLS ATTENDED:

University of Oregon, Eugene
Brigham Young University, Provo, Utah
Olympic College, Bremerton, Washington

DEGREES AWARDED:

Doctor of Philosophy, Chemistry, 2012, University of Oregon
Bachelor of Science, Physics, 2007, Brigham Young University

AREAS OF SPECIAL INTEREST:

Cytoskeleton and motor proteins

Protein biochemistry

ACKNOWLEDGMENTS

I would first like to express my sincere appreciation of my advisor, Dr. Ken Prehoda, for his mentorship and advice throughout this work. I am deeply grateful for his guidance throughout the development of this project and my development as a scientist. I would also like to thank my fellow lab members both current and past, who made my work so enjoyable over the last few years. I would particularly like to thank Derek Ricketson for his help in developing this project in its early stages and training me in the specialized techniques used. This investigation was funded by grant number R01 GM068032 from the National Institutes of Health awarded to Dr. Ken Prehoda.

To my parents who instilled the love of learning in me from an early age
and to my wife who has loved and supported me untiringly

TABLE OF CONTENTS

Chapter Page

Chapter Page

LIST OF FIGURES

Figure Page

CHAPTER I

INTRODUCTION

One of the most basic necessities in biology is the need for motion. This need is visible in nearly all biological systems, where objects must move toward or away from each other in order for processes to occur. Enzymes must be able to find and bind their substrates, and then release them so they can diffuse away. Cells of all types and sizes need nutrients and energy in order to survive, which must be moved into and around the cell. In order for reproduction to occur, cells must be able to move away from their offspring. Specific motions are needed for life to exist.

At extremely small scales simple random diffusion fills the need for motion. Enzymes rely almost exclusively on diffusion for movement of substrates into and out of active sites. Bacterial cells are almost completely powered by random diffusion within their cytoplasms that move things around. At those small scales and at typical temperatures thermal diffusion can power the necessary reactions. However, as the size scale increases, diffusive Brownian motion decreases. Thus at larger scales, diffusion becomes increasingly inefficient as a source of locomotion. Inputting energy randomly into the system only helps the situation marginally, since this will only serve to increase the frequency of random encounters. Diffusion-based systems run up against the

fundamental rule that they can do nothing that change the probability that the desired encounters will occur.

This problem is solved, and efficiency is greatly improved by the ability of eukaryotes to direct their movement toward desired targets. With directed locomotion, useful encounters can be selected and driven to occur more often. Objects within the cell can be segregated, allowing specialization among the organelles within cells. Cells can be differentiated into niches to form multicellular organisms. Morphogenesis in larger organisms requires directed motion to specify which components end up in which cells and parts of cells. For these reasons, all eukaryotes have a complex cytoskeleton that allows them to direct motion within the cells and motility of the entire cell.

Roles and Elements of the Cytoskeleton

The eukaryotic cytoskeleton gives the cells structure and provides "tracks" within the cell and engines that move along those tracks. Three types of filaments characterize the cytoskeleton: microtubules, intermediate filaments, and actin filaments. Microtubules are thick tubes made up of two proteins arranged in such a way as to provide a rigid, dynamic structure within the cell. They grow in a stereotyped fashion from one end (the plus end). Intermediate filaments are somewhat thinner and come in several different varieties. They are grouped together primarily by their similarity in appearance, and are typically much more flexible than microtubules. The last type of filament, the actin filament, is composed of just one protein: actin. Like microtubules, actin filaments are quite stiff and provide a rigid, dynamic substrate for the cell. They

also grow predominantly in one direction. The direction of growth is known as the "barbed" end, while the opposite end is the "pointed" end due to the conformations of these ends of the filaments.

Each of these types of filament has distinct roles, although their roles somewhat overlap. Microtubules can grow and shrink to provide force within the cells, and give structure to cellular projections such as flagella and cilia. They can also act as a scaffold for trafficking things around the cell, providing a structure for trafficking vesicles and organelles around the cell. One of their most well known roles is to separate replicated DNA during anaphase of mitosis.

Intermediate filaments support the three-dimensional shape of the cell by supporting the cellular membrane and keeping certain organelles positioned inside of the cell.

Actin filaments have a diverse set of roles. Like microtubules, they can act as a track for trafficking things around the cell and supporting the cellular membrane. Actin filaments come in a variety of arrangements. At the cellular cortex actin filaments form a complex web of filaments that can change the exterior shape of the cell. Inside the cell the filaments form thick bundles of filaments that both act as a track and transmit forces longer distances within the cell.

Microtubules and actin also have their own motor proteins to use the energy stored in ATP to move along the filaments. Kinesins are a large family of proteins that use ATP to travel along microtubules, primarily toward the growing plus end (Miki et al., 2005). Kinesins are involved with mitosis, meiosis, and organelle transport (Miki et al., 2005; Berg and Hoogenraad, 2012). Dynein is a

much larger complex that moves in the opposite direction, toward to microtubule's minus end, transports organelles, and helps position centrosomes for mitosis (Numata et al., 2008; Gennerich and Vale, 2009). These motors have complementary roles in moving things along the microtubule framework and can act as an anchor. The roles of these motors are mirrored in transport along actin filaments by the family of ATPase motor proteins as myosin.

The Diverse Family of Myosins

Myosins are large family of diverse motor proteins united by the fact that they all bind actin and use the energy stored in ATP to move along actin filaments (Mermall, 1998; Sellers, 1999, 2000). They have typically been identified by the sequence homology of the highly conserved motor domain (Richards and Cavalier-Smith, 2005; Odronitz and Kollmar, 2007). This motor domain is the region of the protein that both binds to actin and hydrolyzes ATP (Dantzig et al., 2006). Carboxyl-terminal of this domain is a neck domain with anywhere from zero to six IQ motifs (Cheney and Mooseker, 1992). IQ motifs bind to EF hand containing proteins such as calmodulin or light chains that are specialized to the functions of their corresponding myosin. Carboxyl-terminal of the neck domain is the tail domain, which has the largest variation among the domains. Its typical role is to anchor and position the motor domain (Geeves and Holmes, 1999). In most myosins the tail also provides a means to interact with the cargo. Additionally, in many myosins the tail domain contains a coiled coil motif that allows interactions that form two-headed dimers.

Despite their commonalities, there is significant heterogeneity within the myosin superfamily that stems from its structural variety (Krendel and Mooseker, 2005). One of the least varying regions within the superfamily is the conserved motor domain. Even in this region, however, there is some variation. The most striking example of this is Myosin VI, has an extra bend between the motor domain and neck that allows it to move in the opposite direction along actin filaments (Nishikawa et al., 2002; Dunn et al., 2010; Spudich and Sivaramakrishnan, 2010). Most myosins move toward to barbed end, while myosin VI moves toward the pointed end. Even with this difference, the actin-binding and nucleotide-binding regions of the motor domain are extremely well conserved.

The neck domains vary in both the number and the types of proteins that bind their IQ motifs. The two primary roles of the neck are to provide a point of regulation of myosin activity and to provide a stiff lever arm to transmit the force of the motor domains to the cargo. Myosins can have as many as six IQ domains (Myosin V) (Houdusse et al., 1996) and as few as none (Myosin XIV) (Soldati et al., 1999). These motifs bind calmodulin in calcium-regulated myosins or the similar specialized light chains in other cases. The length of the neck domain has a large effect on the step size myosins take along actin filaments.

Most of the variation among myosins occurs within the tail domain, with various specialized cargo binding domains and motifs to allow different oligomerization states. Most myosins dimerize by means of coiled coil motifs in their tails, although there are exceptions to this, particularly Myosin IV, which has no coiled coil motif (Horowitz and Hammer, 1990). The length of this coiled

coil varies depending on the role of the myosin from just long enough to form dimers, to over 1000 residues in Myosin II. Myosin tail domains also provide a means of interacting with their cargoes. Based on these tail domains, myosins can have several different types of relationship to the actin filaments that they bind. Several of them, particularly myosin V and myosin VI move cargoes along actin filaments (Kellerman and Miller, 1992; Houdusse et al., 1996). Others, such as Myosin I seem to simply anchor things to filaments (Dai et al., 1999). Myosin II has the unique role among myosins of moving the actin filaments that they bind.

Myosin II moves actin filaments by forming filaments with heads at each end (Niederman and Pollard, 1975). These bipolar filaments move actin filaments past each other (Sellers, 1999). By doing this, myosin II acts as one of the primary sources of intracellular and intercellular contractile force. In skeletal muscles bundles of actin and myosin are arranged in such a way as to provide long-range forces for an organism. These bundles act quickly in response to their regulation by calcium (Ikebe et al., 1994). Smooth muscle provides longer-term force in such places as the digestive tract and blood vessels where constant force is needed. Unlike skeletal muscle, smooth muscle is regulated by phosphorylation of its regulatory light chain (RLC), which binds the neck domain (Sellers et al., 1981; Trybus and Lowey, 1984, 1987).

Non-muscle myosin II (NM-II) is the myosin responsible for providing contractile force to all of the other cells of the body. Non-muscle cells need contraction for cell motility, to maintain cortical tension, and for essential processes like cytokinesis and morphogenesis (Edwards and Kiehart, 1996; May

et al., 1997; Li and Bresnick, 2006; Fischer et al., 2009; Wang et al., 2011). Like other forms of myosin II, NM-II forms bipolar filaments in order to provide contractile force, although NM-II filaments a much smaller than skeletal muscle filaments, and somewhat smaller than smooth muscle filaments (Citi et al., 1987; Craig and Woodhead, 2006).

Myosin II Force Production

The production of force by all myosins is similar due to the high level of conservation in the motor domain. The motor domains are composed of four subdomains (Houdusse et al., 1999). The amino-terminal subdomain binds actin at an SH3-like motif (Dominguez et al., 1998), with additional binding contacts being made in the cleft between the upper and lower 50 kDa subdomains of the motor domain. The contacts in the cleft between the 50 kDa subdomains are dependent on nucleotide binding, which allows myosin to produce its force (Rayment et al., 1993a).

The myosin nucleotide binding pocket is located in the lower 50 kDa subdomain. ATP binds the nucleotide in this pocket when it is bound to actin (Rayment et al., 1993b, 1996). ATP binding causes a slight conformational shift that allows dissociation from the actin filament. Then when ATP hydrolyzes into ADP and inorganic phosphate the motor domain shifts forward along the actin filament in what is known as the "recovery stroke." The ADP-Pi bound motor domain then binds a new position along the actin filament, causing the release of the inorganic phosphate. When the inorganic phosphate is released another conformational shift occurs, forcing the actin filament backward in what is

referred to as the "power stroke." Once it is in this conformation ADP can be released and the cycle is started again (Dominguez et al., 1998; Tyska and Warshaw, 2002; Elber and West, 2010).

Some myosins, such as myosin V, which is known as a processive motor, have at least one head of the dimer bound to the actin filament at all points in their ATPase cycle (Moore et al., 2001). The fraction of the time the motor spends bound to actin is know as its “duty ratio” and in order to walk in a hand-over-hand fashion along actin filaments, myosin V must have a high duty ratio. Processivity is an essential attribute of myosin V if it is to continue along actin filaments (Tyska and Mooseker, 2003).

Myosin II, on the other hand, is a non-processive motor, meaning that there are points in the cycle where neither head of the dimer is attached to actin. Its non-processivity is a result of it being a low duty-ratio motor, meaning that a low fraction of its cycle is spent bound to actin. Myosin II function is intrinsically tied to the formation of bipolar filaments. These filaments contain multiple dimers oriented to have motor domain heads on both ends (Niederman and Pollard, 1975). They are spaced in such a way as to distribute the motor domains over the actin filament tracks. In this fashion, individual dimers can be non-processive, while maintaining processivity of the filament as a whole.

Bipolar filament assembly occurs by means of a roughly 90-residue region near the C-terminus of the coiled-coil tail of NM-II (Liu et al., 2008). It has been shown that complementary charges in this region cause filaments to associate, and dictate the spacing of the individual dimers within the filament, and

disruption or changes to these charges cause different arrangements of the bipolar filaments (Hostetter et al., 2004; Ricketson et al., 2010).

Non-Muscle Myosin II Regulation

Unregulated ectopic force could cancel out the directed forces needed for completion of essential cellular processes. Hence, regulation of activity and localization of NM-II is essential. This raises the question of how NM-II is activated at the proper time and place that contractile force is needed and turned off when unneeded (Sellers and Knight, 2007). Regulation of myosin II is centered at the neck domain (Adelstein and Conti, 1975; Craig et al., 1983). In smooth muscle and non-muscle myosin II, two light chains bind the two IQ motifs in the neck. The amino-terminal one is known as the essential light chain (ELC) and has no known role aside from stiffening the neck lever arm (Dominguez et al., 1998; Quevillon-Cheruel et al., 2000; Kazmierczak et al., 2009). The carboxyl-terminal one is called the regulatory light chain (RLC), and is the linchpin for regulation of the entire dimer (Craig et al., 1983; Trybus and Lowey, 1984; Citi et al., 1987).

The RLC is an EF hand protein that mostly wraps around the IQ motif of the heavy chain and has a short an amino-terminal extension (Dominguez et al., 1998). This amino-terminal extension is phosphorylated at two adjacent positions: a serine and a threonine, which leads to the regulation of the entire complex (Kamisoyama et al., 1994). It is phosphorylated at both positions by Rho kinase in *Drosophila* and by a set of related kinases in mammals (Ueda et al., 2002; Yamashiro et al., 2003; Dean and Spudich, 2006). It inactivated when it is

dephosphorylated by myosin phosphatase (Ito et al., 2004; Matsumura et al., 2011). Phosphorylation of both residues is essential for full activity of the motor domain (Ueda et al., 2002; Mizutani et al., 2006).

When the RLC is unphosphorylated the dimers are unable to form the bipolar filaments necessary for force production and the motor domains are inactive (Citi et al., 1987). The most striking feature of the autoinhibited NM-II is the coiled-coil tail or rod domain, which folds back on itself twice (Craig et al., 1983; Trybus and Lowey, 1984). This conformation is quite compact, which has been suggested to help the inactive dimer diffuse more quickly within the cell (Cross, 1988; Breckenridge et al., 2009). Prior to the work described in this Dissertation, it was unknown whether filament assembly was inhibited by direct interaction with the assembly domain or by steric hindrance caused by the folding up of the rod.

In inactive NM-II, the motor domains fold back and shut down, forming a series of stereotyped contacts between the two heads (Dominguez et al., 1998; Burgess et al., 2007). In this conformation there is almost no enzymatic activity. It is not clear by what means the RLC causes the motor domains to fold back. However, it has been demonstrated that only the amino-terminal region of the coiled-coil rod is necessary for autoinhibition of motor domain activity, so motor domain inactivation is not dependent on filament assembly inactivation (Trybus et al., 1997). The converse has not been shown, and it is an open question how RLC phosphorylation causes folding up of the tail domain.

Outside of the canonical RLC diphosphorylation there are several other less well-understood means of regulation. On the amino-terminal extension of

the RLC there are several other phosphorylation sites by kinases known to be associated with cytokinesis that do not seem to regulate NM-II directly (Nishikawa et al., 1984). Additionally, multiple phosphorylation sites on the heavy chain around the assembly domain and the carboxyl-terminal non-coiled coil tailpiece have been shown to have some effects on filament assembly rates (Conti et al., 1991; Dulyaninova et al., 2005; Even-Faitelson and Ravid, 2006; Ludowyke et al., 2006; Clark et al., 2008; Wang et al., 2011). Aside from post-translational modifications, other regulatory mechanisms include proteins that are known to bind the heavy chain, particularly S100A4, a small EF hand protein that binds near the assembly domain and disrupts NM-II activity (Garrett et al., 2006; Li and Bresnick, 2006; Kiss et al., 2012).

Relationship of NM-II Heavy Chain Structural Elements to Regulation

The number of potential pathways of regulation suggests that NM-II regulation is quite complex. Indeed, despite years of study a mechanistic understanding of the regulation has not yet been reached. The approach I have taken in studying this problem has been to investigate regulation by determining the structural elements necessary for autoinhibition of filament assembly.

The contacts made between the motor domain, RLC and rod have been approximated by fitting crystal structures of the active motor domain into cryo-EM micrographs (Liu et al., 2003; Sheng et al., 2003; Burgess et al., 2004). The contacts predicted in these models have also been tested with photo-cross linking, lending support to the models (Offer, 1990; Salzameda et al., 2006). The path of the tail in its folded state and as it passes around the inactive motor domain has

also been approximated by cryo-EM and cross-linking (Burgess et al., 2007). However, these structures are estimated and the precise contacts that stabilize the autoinhibited conformation are still unknown.

It is known that the neck and its IQ motifs are necessary for autoinhibition. However, work in *S. pombe* showed that deletion of the RLC resulted in complete inactivation of NM-II, while deleting the second IQ motif resulted in constitutive activation (Naqvi et al., 2000). This suggests that the IQ domains play some role in autoinhibition. Another region that may play a role in autoinhibition is the non-coiled coil tailpiece, which has been reported previously to play a role in the level of filament assembly and is phosphorylated at several points (Hodge et al., 1992; Ronen and Ravid, 2009). In Chapter II of this Work we use analysis by deletion and mutation of the protein sequence in both of these regions and use filament assembly assays, as well as functional assays in S2 cells to isolate small regions that are necessary for autoinhibition of filament assembly. The work described in this chapter was developed and written together with Dr. Derek Ricketson and Dr. Ken Prehoda

The folded up structure of the NM-II coiled coil tail is quite consistent in electron micrographs of the autoinhibited conformation. In order for a coiled coil to fold back on itself as is observed, some sort of hinge must be present in order for predictable bends to form. Analysis of the sequence has revealed several "skip residues" where the structure of the coiled coil deviates from the typical structure and could provide a flexible hinge domain (Offer, 1990; Straussman et al., 2005). Additionally, some have suggested that contacts between different sections of the coiled-coil rod could stabilize the autoinhibited conformation. This bending is

essential for the autoinhibited conformation and is discussed at length in Chapter III. The design of the experiments and the writing of this chapter was performed together with Dr. Ken Prehoda.

Regulation of filament assembly and enzymatic activity, as well as the large-scale conformational shift are all controlled by diphosphorylation of the RLC. It is not clear, though, how these elements are related. Since regulation of the motor domain can occur with only a small part of the tail, a possible model for regulation could be step-wise, i.e. first inhibition of the motor domain, which somehow results in the conformational shift, which inhibits filament assembly. In the work described in this Dissertation we investigate the roles of the various elements of the heavy chain to help illuminate the regulation of this essential protein.

CHAPTER II

CONTROL OF NON-MUSCLE MYOSIN II ASSEMBLY INTO CONTRACTILE FILAMENTS BY ITS IQ AND TAILPIECE MOTIFS

The experiments described in this chapter were designed in collaboration with Dr. Derek Ricketson and Dr. Kenneth E. Prehoda. Dr. Prehoda also contributed to the writing and editing of this chapter.

Introduction

Contractile force generation by non-muscle myosin II (NM-II) originates from its assembly into structures known as bipolar filaments with motor domains positioned at either end (Niederman and Pollard, 1975; Kendrick-Jones et al., 1987). As NM-II filament assembly is necessary for contraction, it is a key regulatory control point. Under non-contractile conditions, myosin II folds into an "autoinhibited" conformation (aka 10S) in which the heavy chain coiled-coil rod assumes a compact form that is not competent for assembly (Trybus et al., 1982). Contraction is activated by regulatory light chain phosphorylation, which causes unfolding of the rod into an extended form (aka 6S) that oligomerizes to form the bipolar minifilament (Craig et al., 1983; Trybus and Lowey, 1984). Although the folded NM-II 10S conformation has been studied by electron

microscopy (Liu et al., 2003; Salzameda et al., 2006; Burgess et al., 2007), little is known about which elements stabilize this regulatory conformation.

NM-II bipolar filaments are stabilized by interactions between the coiled-coil tail domains of dimerized NM-II heavy chains (Lowey et al., 1969; Craig and Woodhead, 2006). In filaments, the tail forms a long, extended structure that interacts with other tail domains, predominantly through electrostatic interactions, to form overlapping parallel and anti-parallel contacts (Nakasawa et al., 2005; Ricketson et al., 2010). In the autoinhibited globular structure, however, several bends in the tail domain cause it to fold over the neck domain between the motor domain and coiled-coil tail (Craig et al., 1983). Tail domain folding eliminates filament formation (Citi and Kendrick-Jones, 1987), indicating that under non-contractile conditions, the stability of intramolecular contacts is higher than that of intermolecular ones.

Autoinhibited NM-II is activated by phosphorylation of the regulatory light chain (RLC) (Craig et al., 1983; Trybus and Lowey, 1984). In the unphosphorylated state, the RLC NH_2-terminus is unstructured, but assumes an α-helical conformation upon phosphorylation (Nelson et al., 2005). How RLC phosphorylation causes filament assembly, switching from a state that favors intramolecular interactions over intermolecular ones, is not known, however. One impediment for understanding NM-II activation is the lack of understanding of the critical interactions that stabilize the autoinhibited conformation. Without knowing which elements are critical for stabilizing intramolecular contacts, it is difficult to describe the activation process. We set out to remedy this situation by

identifying the minimal components of NM-II that are required to inhibit filament assembly.

Results

The Motor Domain and Light Chains Are Dispensable for NM-II Autoinhibition

The rod domain of the NM-II heavy chain contains an assembly domain (AD) that mediates bipolar filament assembly (Craig and Woodhead, 2006). We identified NM-II regulatory components by determining which AD-containing NM-IIs do not form filaments. The overall architecture of NM-II is shown in Fig. 1A,B, with two light chains and a heavy chain that can be divided into motor, neck, and rod domains (the AD is contained within the rod domain). For our analysis, we used *Drosophila* NM-II as we have extensively characterized its AD (Liu et al., 2008; Ricketson et al., 2010), and it is highly similar to other metazoan NM-IIs. Our strategy was to identify a minimal NM-II that contains the AD (and is thus capable of filament assembly) but does not form filaments.

We first examined whether the motor domain of the heavy chain and the two light chains are required to inhibit filament assembly. The ELC and RLC subunits bind to short IQ motifs in the "neck" of the heavy chain (Fig. 1A). We purified an NM-II protein containing the entire tail and rod domain of the heavy chain, but lacking the motor domain and light chains. We replaced the motor domain with GFP as the presence of a globular domain at the start of the heavy chain promotes the formation of minifilaments rather than paracrystals (Chowrashi and Pepe, 1977; Bennett, 1981). To determine the extent of filament assembly, we used a salt-dependent pelleting assay that has been used

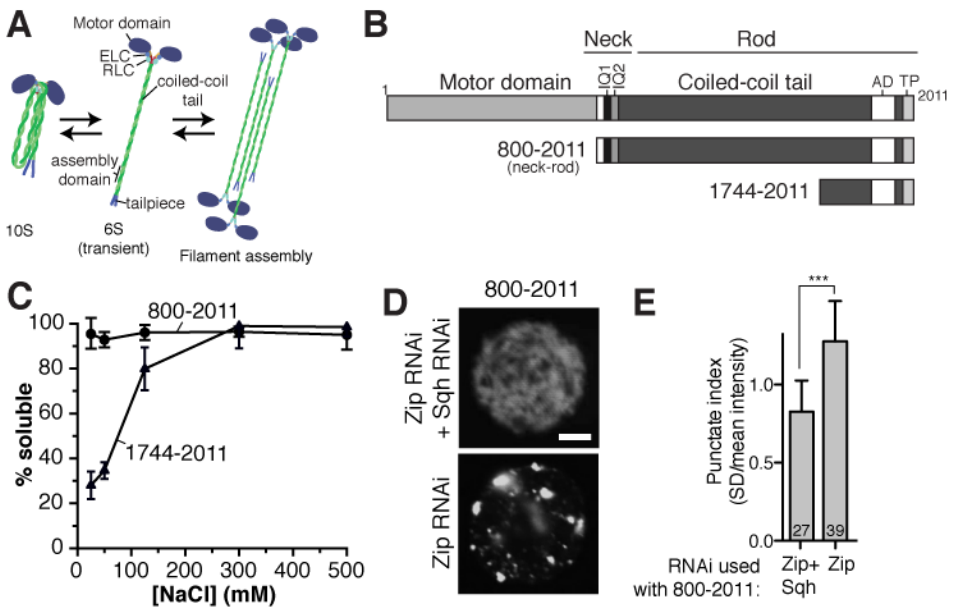

Figure 1. Regulation of non-muscle myosin II filament assembly in the absence of the light chains and motor domain. (A) Non-muscle myosin II regulation. The 10S form assumes a compact conformation that lacks motor domain ATPase activity and the ability to form filaments. Phosphorylation of the regulatory light chain (RLC) induces formation of the 6S form that is competent to assemble into bipolar filaments. (B) The NM-II variants analyzed for autoinhibition. Abbreviations: Assembly domain (AD), Tailpiece (TP). (C) Quantification of the solubility properties of the truncations of panel B determined by salt-dependent pelleting assays of the fragments. The truncation containing the neck domain but not the motor domain or light chains does not form filaments, as assessed by this assay. Both proteins were assayed at a concentration of 200 nM. Error bars represent one SD from three independent measurements. (D) Residues 800-2011 form large puncta in S2 cells, which is indicative of filament assembly (Liu et al., 2008; Uehara et al., 2010). When RLC (Sqh) is inactivated by RNAi, the localization is diffuse, characteristic of monomeric, non-filamentous NM-II. (E) Quantification of cell images. The values shown represent the standard deviation of pixel intensity divided by the mean intensity in the cytoplasm. Statistical significance was evaluated using a t-test (*** denotes $p < 0.001$). The number of cells analyzed is shown in each bar.

extensively to detect myosin II filament formation (Nakasawa et al., 2005; Ricketson et al., 2010). This assay takes advantage of the high molecular weight of myosin II filaments that allows them to be separated from soluble monomers by ultracentrifugation. Filament stability is electrostatic in nature and highly dependent on ionic strength such that assembly is highly favored at 100 mM NaCl but at 250 mM NaCl the effects of ionic screening cause disassembly.

Using the salt-dependent pelleting assay, we found that the heavy chain neck-rod (residues 800-2011) does not form filaments, despite containing the filament assembly domain (Fig. 1C). As we have found previously (Liu et al., 2008), a COOH-terminal portion of the rod domain that contains the AD (residues 1744-2011) readily forms filaments (Fig. 1C). The heavy chain neck-rod contains the AD but does not assemble into filaments, indicating that autoinhibitory elements lie within this sequence. Thus, the motor domain and light chains are not necessary to inhibit filament formation.

To test the behavior of the heavy chain neck-rod in a cellular context, we expressed it in cultured *Drosophila* S2 cells. NM-IIs that assemble into filaments have been shown to form punctae in S2 cells, whereas monomers are diffuse throughout the cytoplasm (Liu et al., 2008; Uehara et al., 2010). We used RNAi to prevent the expression of endogenous RLC and heavy chain. In this background, the neck-rod remained diffuse (Fig. 1D,E), consistent with our observation that it does not filament *in vitro*. Interestingly, in cells that still contained the RLC, the neck-rod formed distinct punctae (Fig. 1D,E), indicating

that the presence of the RLC overcomes the regulation present in the neck-rod to allow filaments to assemble.

Position-Dependent Regulatory Elements Within the Coiled-Coil Tail

The coiled-coil tail constitutes over three-quarters of the residues in the neck-rod and forms the interaction surface for filament assembly. The assembly domain resides at the COOH-terminal end of the tail so we used internal deletions to determine the extent to which regions outside of the assembly domain regulate filament formation. As shown in Fig. 2, the pattern of filament assembly for these deletions is complex. Deletion of residues between the neck and residue 1725 disrupted regulation leading to filament formation (Fig. 2B,C), whereas deletion to residues 1735 to 1785 remained regulated (Fig. 2D). Further deletion to the assembly domain (residue 1849) again led to a loss of regulation and formation of filaments (Fig. 2E). Thus, only approximately 100 residues NH_2-terminal to the AD are required for filament regulation, but other deletions can disrupt regulation.

The pattern of regulation in coiled-coil tail deletions suggests that the interactions that regulate filament assembly must be maintained in a particular register in order to stabilize the autoinhibited conformation. In electron microscopy images of autoinhibited NM-II the tail folds back upon itself, which is likely to position elements that stabilize the structure next to one another. Thus, certain deletions could disrupt the register of these interactions, whereas others

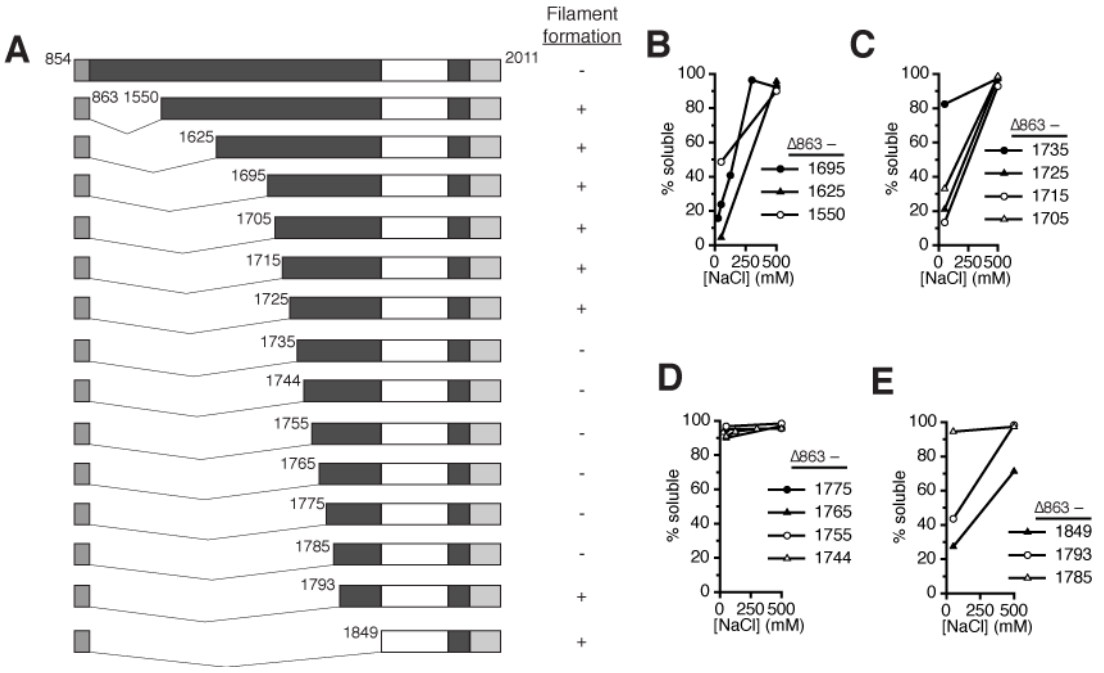

Figure 2. A specific region of the coiled-coil tail that includes the assembly domain is required to maintain autoinhibition by the neck domain. (A) Schematic of internal deletions of the coiled-coil tail region. (B-E) Salt-dependent pelleting assays demonstrating the region of the coiled-coil tail that is necessary for autoinhibition.

may be compatible with regulatory element interaction and inhibition of filament assembly.

Neck Domain IQ Motifs Redundantly Regulate Filament Assembly

The neck domain sits between the motor and tail domains and contains the light chain binding sites (Fig. 1B). Deletion of the entire neck domain, leaving only the rod (residues 884-2011), leads to filament assembly as assessed by its salt-dependent pelleting behavior (Fig. 3B). Consistent with its *in vitro* behavior, the rod forms discrete puncta when expressed in S2 cells (Fig. 3C,D). Unlike the full neck-rod, RLC RNAi had no effect on the localization pattern of the rod, consistent with the presence of the light chain binding domains within the neck. We conclude that the neck domain is required for filament regulation.

We next examined elements within the neck domain to understand how it contributes to filament regulation. The neck contains two IQ motifs, IQ_1 and IQ_2, which bind the ELC and RLC, respectively. We removed each IQ motif individually and observed no effect on filament assembly (Fig. 3B-D). Removal of either IQ_1 or IQ_2 does not restore filament assembly *in vitro* and in S2 cells the IQ_2 domain of the neck is sufficient to maintain the diffuse, autoinhibited phenotype (Fig. 3C-E). In contrast to the individual removal of the IQ motifs, deleting both IQ_1 and IQ_2 induced filament assembly (Fig. 3B). The requirement for either one of the IQs indicates that the motifs redundantly regulate filament formation.

We isolated 10-residue regions within the IQ motifs that are sufficient for autoinhibition (Fig. 3F,G). This sequence, which shares a high degree of

Figure 3 (next page). Ten residue sequences within the neck IQ motifs redundantly regulate filament assembly. All proteins were assayed at a concentration of 10 ìM unless otherwise indicated. All error bars represent one SD of three independent measurements. (A) Schematic of the NM-II variants used to analyze the role of neck region. Two 10-residue regions of the neck, one in each IQ motif, are sufficient to inhibit filament assembly. Abbreviations: Assembly domain (AD), Tailpiece (TP). (B) Pelleting assays demonstrating that inclusion of the second IQ motif (854-2011) is sufficient to inhibit filament assembly, while removing the entire neck domain (884-2011) results in filament formation. Both proteins were assayed at a concentration of 200 nM. (C, D) Representative images and quantification of images showing that inclusion of the neck domain results in diffuse localization in the absence of the RLC (Sqh), while the coiled-coil tail alone remains punctate. Statistical significance was evaluated using one-way analysis of variance followed by Dunnett's post test using 800-2011 with Zip (heavy chain) and Sqh inactivated by RNAi as a control group (*** denotes $p<0.001$) The number of cells analyzed is shown in each bar. (E) Pelleting assays of deletions within the neck domain. Either of the IQ domains is able to inhibit filament assembly. (F) Deletions within the first IQ domain showing that the residues 828-837 are able to cause autoinhibition, while the rest of the domain cannot. (G) Deletions within the second IQ domain showing that the residues 854-863 are essential for autoinhibition. (H) Structural model of the neck domain. The regions of the neck domain that are necessary for autoinhibition are mapped onto a crystal structure of scallop smooth muscle myosin regulatory domain (PDB: 3PN7). The ELC is shown in grey, the RLC in cyan, and the heavy chain in yellow with the essential 10-residue regions of both IQ domains highlighted in blue. In the structure, the essential residues of the IQ_1 domain are nearly completely buried by the ELC, while the essential 10 residues of the IQ_2 domain remain exposed when the RLC binds. (I) Multiple sequence alignment showing conservation within the neck domain. The residues found to be most important for autoinhibition are marked in red. (J) Alanine-scanning point mutations within the region Residues 854-863. The residue with the greatest impact on autoinhibition is C861, with I854, I856, and Q858 having a lesser impact. Mutation of Cys-861 to serine has a similar impact to a mutation to alanine. (K) The residues R855, I857, R859, and N860 had very little impact on autoinhibition when mutated to alanine, as assessed by salt-dependent pelleting.

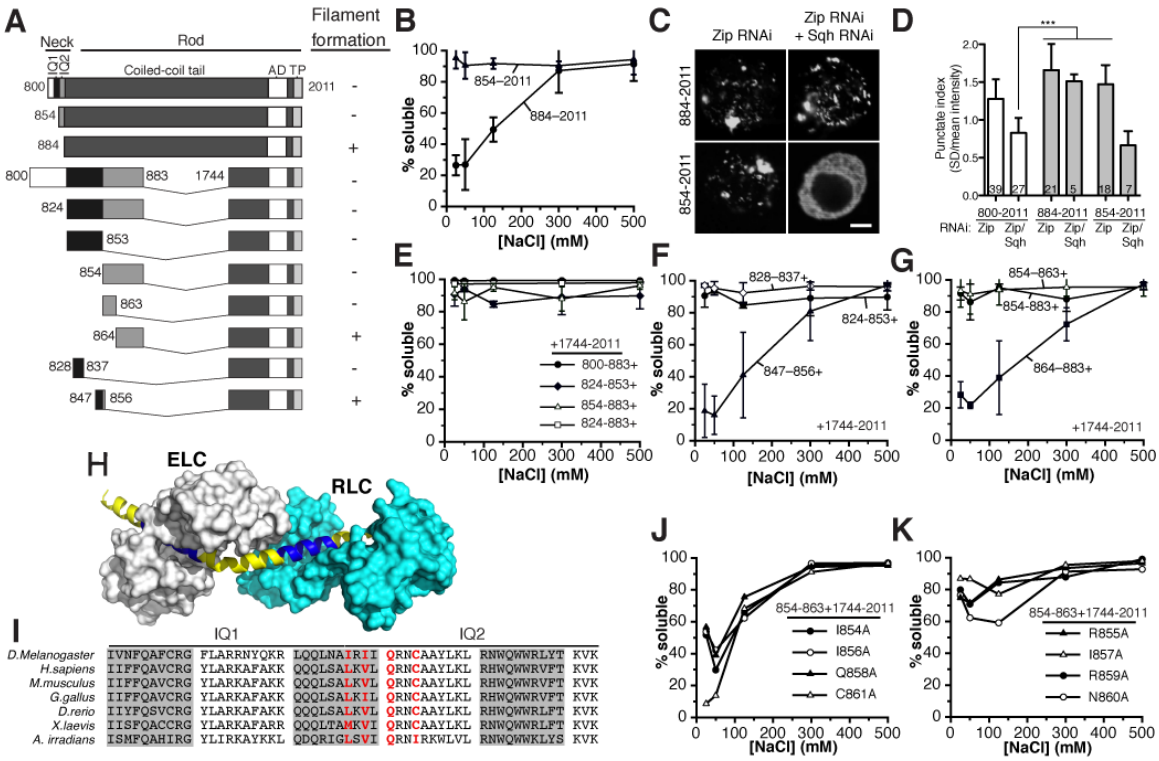
A
Neck
Rod
IQ1
IQ2
Coiled-coil tail
AD
TP
Filament formation
800
2011
854
884
883
1744
824
853
863
864
828
837
847
856
B
% soluble
854–2011
884–2011
[NaCl] (mM)
C
Zip RNAi
Zip RNAi + Sqh RNAi
884-2011
854-2011
D
Punctate index (SD/mean intensity)
***
800-2011
884-2011
854-2011
RNAi: Zip Zip/ Sqh Zip Zip/ Sqh Zip Zip/ Sqh
39 27 21 5 18 7
E
+1744-2011
800-883+
824-853+
854-883+
824-883+
F
828–837+
824-853+
847–856+
+1744-2011
G
854–863+
854-883+
864–883+
+1744-2011
H
ELC
RLC
I
IQ1
IQ2
D.Melanogaster IVNFQAFCRG FLARRNYQKR LQQLNAIRII QRNCAAYLKL RNWQWWRLYT KVK
H.sapiens IIFFQAVCRG YLARKAFAKK QQQLSALKVL QRNCAAYLKL RHWQWWRVFT KVK
M.musculus IIFFQAVCRG YLARKAFAKK QQQLSALKVL QRNCAAYLKL RHWQWWRVFT KVK
G.gallus IIFFQAVCRG YLARKAFAKK QQQLSALKIL QRNCAAYLKL RHWQWWRVFT KVK
D.rerio IIYFQSVCRG YLARKAFAKK QQQLSALKVL QRNCAAYLKL RHWQWWRLFT KVK
X.laevis IISFQACCRG YLARKAFARR QQQLTAMKVI QRNCAAYLKL RNWQWWRLFT KVK
A. irradians ISMFQAHIRG YLIRKAYKKL QDQRIGLSVI QRNIRKWLVL RNWQWWKLYS KVK
J
854-863+1744-2011
I854A
I856A
Q858A
C861A
K
854-863+1744-2011
R855A
I857A
R859A
N860A
% soluble
[NaCl] (mM)

sequence similarity between the two IQs and is an integral part of the light chain contact interface (Fig. 3H) prevents assembly of the 1744-2011 region, while other neck segments do not (Fig. 3F,G). Alanine-scanning mutagenesis within the 10-residue segment of IQ_2 revealed several residues, including C861, I854, I856, and Q858, that are critical for filament regulation (Fig. 3J,K). These data suggest that the neck interactions that stabilize the autoinhibited conformation of NM-II are specific to a small number of residues within the IQ motifs of the neck domain.

A Short, Conserved Region of the COOH-Terminal Tailpiece Is Required for Autoinhibition

To determine if regions COOH-terminal to the assembly domain might be needed for autoinhibition, we deleted the tailpiece, a short (residues 1969-2011), non coiled-coil region at the end of the heavy chain. Using the salt-dependent pelleting assay, we found that deleting the tailpiece resulted in complete rescue of filament formation, indicating a requirement for the tailpiece in filament regulation (Fig. 4B). When expressed in S2 cells, the neck-rod lacking the tailpiece forms robust puncta further confirming filament assembly (Fig. 4C,D). We conclude that, in addition to an IQ motif from the neck domain, the tailpiece is required for regulating filament assembly.

To determine which elements within the tailpiece are necessary for autoinhibition, we performed a deletion analysis. We found that truncating the tailpiece from the COOH-terminus beyond residue 1988 results in complete restoration of filament assembly (Fig. 4A,E-F). We then performed several

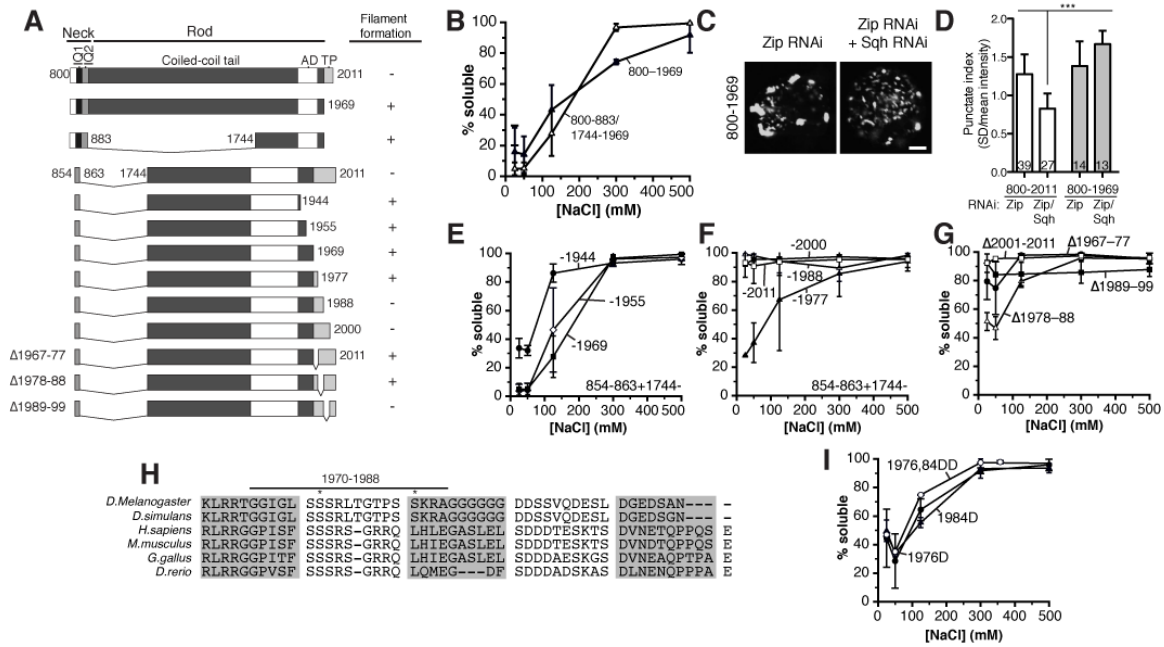

Figure 4. Analysis of the autoinhibitory regions of the COOH-terminal tailpiece. All proteins were assayed at a concentration of 10 ìM unless otherwise indicated. All error bars represent one SD of three independent measurements. (A) Schematic of NM-II variants used to analyze the tailpiece. Residues 1967-88 are necessary for autoinhibition. Abbreviations: Assembly domain (AD), Tailpiece (TP). (B) Deleting the tailpiece (Residues 1970-2011) eliminates autoinhibition, even in the presence of the neck domain. These proteins were assayed at a concentration 200 nM. (C) S2 cell transfections of the NM-II neck and rod without the tailpiece (Residues 800-1969). Unlike fragments that encompass the entire neck and tail, these fragments localize to punctae in the cell, even in the absence of the RLC (Sqh). (D) Quantification of S2 cell localization. (E, F) Truncations of the tailpiece show that deleting beyond Residues 1988 completely restores filament assembly. (G) Deletions within the tailpiece show that filament assembly is somewhat increased by deletions of both Residues 1967-77 and Residues 1978-88. (H) Multiple sequence alignment showing conservation within the tailpiece. (I) Phosphomimetic point mutations of phosphorylatable residues restore filament assembly.

internal deletions within the tailpiece, and found that deleting residues 1978-88 substantially restored filament assembly (Fig. 4G), supporting a role for this region in regulating filament assembly. Removal of residues 1988-2011, however, had no effect on filament assembly of the neck-rod. From this analysis we conclude that residues 1970-1988 are the regulatory elements within the non-coiled coil tailpiece.

Although much of the tailpiece is poorly conserved, residues 1970-1981 are highly conserved among insects and vertebrates (Fig. 4H) suggesting that filament regulation by the tailpiece is a conserved function. It has also been reported that several residues within the tailpiece are phosphorylated (Breckenridge et al., 2009). We found that mutating the phosphorylated residues S1976 and S1984 to phosphomimetic glutamic acid resulted in complete restoration of filament assembly (Fig. 4I) suggesting that tailpiece phosphorylation may play a role in regulating filament assembly.

Minimal Autoinhibited Myosin II Forms a Compact Structure That Extends Upon Activation

Autoinhibited full-length NM-II assumes a more compact conformation than the activated form. This was first detected by analytical ultracentrifugation (AUC), and resulted in the autoinhibited and activated conformations being referred to as the 10S and 6S conformations, respectively (Craig et al., 1983). Although significantly smaller than full length NM-II, we performed AUC on a minimal regulated heavy chain that we identified (10 residues from IQ_2 fused to residues 1744-2011), to determine if we could detect a size difference upon

activation. We compared the hydrodynamic characteristics of the minimal autoinhibited NM-II, as determined by sedimentation velocity AUC, to forms where the autoinhibition is disrupted. We observed a decrease in the sedimentation coefficient for NM-IIs that aren't autoinhibited (Fig. 5A). Although small, the shift is highly statistically significant and is consistent with a conformational change of a protein of this molecular weight. The conformational change suggests that inhibition of filament assembly in these minimal fragments occurs concomitantly with a conformational change, as is the case with the full-length NM-II.

An IQ Peptide Activates Autoinhibited Myosin II

How do the NM-II elements that we have identified regulate filament assembly? To answer this question, we determined if the IQ motif affected filament assembly of the minimal regulated NM-II when added *in trans*. Competition between *cis* and *trans* IQ motifs could maintain repression if the *trans* IQ was sufficient for inhibition. Alternatively, replacement of the *cis* IQ with the *trans* one could induce filament assembly if covalent linkage of the IQ with the rest of the protein were required for regulation. As shown in Fig. 5B, we observed robust activation of the normally inhibited IQ_2-1744-2011 fusion when a peptide containing the first 10 residues of the IQ_2 motif was added *in trans*. Addition of a control peptide (the PDZ ligand from the protein Stardust (Peterson et al., 2004)) had no effect, indicating that the effect is specific to the IQ sequence. Thus, the *in trans* IQ motif disrupts the intramolecular regulatory interaction, and the interaction that replaces it is not sufficient to inhibit filament assembly.

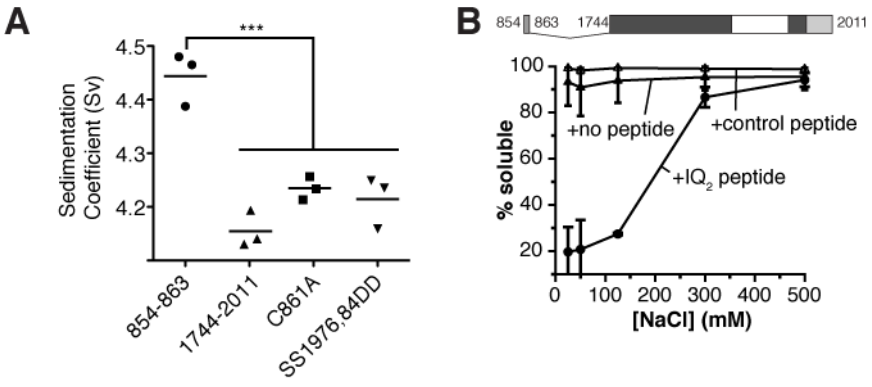

Figure 5. Conformational analysis of short autoinhibited fragments by analytical ultracentrifugation and salt-dependent pelleting assays. (A) The fragments with and without the 10-residue core of the IQ motif were centrifuged at 50,000 rpm at 20˚C and their traces analyzed with Sedfit. Each of these fragments contained the mutation K1912E that has been previously shown to eliminate filament assembly, preventing higher-weight oligomers from forming. The analysis was repeated three times for each mutant or fragment, and the peaks were integrated using the Sedfit software to find the average sedimentation coefficient. The mean of the three runs is indicated with a bar. Statistical significance was evaluated using one-way analysis of variance followed by Dunnett's post test using 854-863 as a control group (*** denotes $p < 0.001$). (B) Filament assembly assays of the construct 854-863 with a peptide consisting only of residues 854-863 at 50 μM, a control peptide from the D. melanogaster Sdt gene at 50 μM, or no peptide. The IQ peptide is able to completely restore filament assembly. Error bars represent one SD of three independent measurements. Both the analytical ultracentrifugation and the pelleting assay were conducted with 10μM NM-II protein.

We conclude that folding of the tail domain, mediated by interactions with the IQ motif, inhibits NM-II filament assembly but not by direct interference with interactions that stabilize the filament.

Discussion

Autoinhibition is a common regulatory mechanism in which functional components and their controlling elements lie within the same structure, and interactions between these elements repress activity (Pufall and Graves, 2002). Activation can occur by mechanisms that interfere with the intramolecular interactions such as direct binding or post-translational modification. The large-scale conformational shift of the actin motor protein non-muscle myosin II (NM-II) provides a dramatic example of autoinhibition. In its autoinhibited state, NM-II's long coiled-coil tail intricately folds back on itself several times and when it is activated it assumes an extended conformation (Craig et al., 1983). It then is able to perform its function of generating contractile forces in the cell. These forces must be highly regulated spatially and temporally to provide the force necessary for processes such as cell motility and cytokinesis (Craig and Woodhead, 2006; Sellers and Knight, 2007; Ikebe, 2008; Milton et al., 2011).

In this study we have investigated the elements of NM-II that are necessary for inhibition of filament assembly. Based on our data, we are able to eliminate the light chains as participants in autoinhibition in *Drosophila* NM-II. However, half of the residues that constitute the light chain binding sites (IQ motifs) are required to inhibit filament assembly, and these two sequences act redundantly to control filament assembly. The IQ motifs have been implicated in

regulation of *S. pombe* NM-II although the mechanism was unclear (i.e. regulation of motor activity or filament assembly). We propose that the IQ domains are critical participants in controlling NM-II filament formation. The high degree of conservation between *Drosophila* NM-II and vertebrate proteins, along with the requirement for IQ in *S. pombe* NM-II regulation, raises the possibility that a similar autoinhibitory mechanism occurs in evolutionarily distant eukaryotes.

Although the light chains are not required for autoinhibition, phosphorylation of the RLC activates filament assembly. The coupling between RLC and IQ motifs is likely to be important for transducing RLC phosphorylation into filament formation. This conclusion is lent some support by crystal structures of the neck domain of the closely related smooth muscle myosin (Houdusse et al., 1999; Kumar et al., 2011). In these structures the ELC completely engulfs the first IQ motif, making any contact between the motif and any other region of the heavy chain seem unlikely, but in crystal structures of the active form the second IQ motif is somewhat exposed. Although the phosphorylated NH_2-terminal residue is not resolved, these residues are thought to be quite disorderly in the active state, making it seem unlikely that they could be completely blocking access to the IQ_2 motif.

We have also identified the COOH-terminal tailpiece as a critical player in filament inhibition. This is somewhat surprising in light of current structural models of the autoinhibited conformation, which place the tailpiece at the opposite end of the protein from the RLC and neck domains. The tailpiece is on of the most variable regions of myosin II between isoforms, and several studies

have looked at the differences between the isoforms. These studies have shown that the tailpiece affects localization (Breckenridge et al., 2009; Ronen and Ravid, 2009), filament stability (Hodge et al., 1992; Breckenridge et al., 2009), and filament structure (Ronen and Ravid, 2009). Involvement by the tailpiece in autoinhibition is consistent with both localization changes, which is related to filament assembly (Liu et al., 2008), and filament stability stemming from changes in the equilibrium between the activated and autoinhibited conformations. Several phosphorylation and protein-binding sites have also been found in the tailpiece (Li and Bresnick, 2006; Breckenridge et al., 2009; Ronen and Ravid, 2009), and our point mutations in the tailpiece raise the possibility of other modes of regulation aside from RLC phosphorylation.

We also have found that the conformational shift of NM-II is necessary for inhibition of filament formation. While it has long been known that autoinhibition involves a compact structure, it has been unknown whether the conformation or interactions that stabilize it are responsible for filament autoinhibition. The observation that even the most minimal autoinhibited fragment has a conformational shift supports the idea that the shift is necessary for autoinhibition. Further, restoration of filament assembly by a peptide designed to compete away the neck-tail interactions directly shows that the interactions that stabilize the autoinhibited conformation do not inhibit filament formation.

We have focused on the elements of NM-II required for autoinhibition. Understanding these elements is the foundation for a comprehensive model for NM-II regulation, which is critical in many cellular contexts. Several other

aspects remain to be addressed, including tail-tail interactions, the role of flexible hinge regions, and how the inhibition of filament assembly and motor domain activity is connected. However, an understanding of the elements that cause formation of the autoinhibited state will allow further efforts to focus on the mechanisms that these elements employ to regulate NM-II activity.

Materials and Methods

Cloning, Over-Expression, and Purification

All of the NM-II fragments were sub-cloned from a plasmid containing full-length Zipper isoform B as previously described (Liu et al., 2008; Ricketson et al., 2010). We created the clones for deletional analysis by overlap extension PCR. All clones were verified by DNA sequencing. Proteins were expressed from the pET-19b derivative pBH vector (Peterson et al., 2004) in *E. coli*, and the proteins were then purified using Ni-NTA resin (Qiagen) using the manufacturer's protocol. In cases where this purification failed to yield >90% pure protein as assessed by SDS-PAGE, the proteins were further purified by ion-exchange chromatography. Purified proteins were dialyzed to a salt-free Tris buffer (20 mM Tris, pH 8.0; 1 mM EDTA; 1 mM DTT) at 4˚ C.

Filament Assembly Assay

The filament assembly assay has been described previously (Liu et al., 2008). Briefly, proteins (at 10 μM unless otherwise noted) were incubated in assembly buffer (20 mM Tris, pH 8.0; 1 mM EDTA; 1 mM DTT) with the appropriate salt concentration at 4˚ C for 30 minutes followed by

ultracentrifugation at 100,000g for 30 min. We then loaded equal volumes of the supernatant and solubilized pellet fractions onto an SDS-PAGE gel for analysis, followed by staining with Coomassie Brilliant Blue. Gels were scanned and the relative amounts in each fraction were quantified with ImageJ (NIH).

Interacting Peptide Filament Assembly Assays

A peptide containing the sequence of the heavy chain neck domain residues 854-863 was synthesized by EZBiolab (Carmel, IN). The desalted peptide was further purified by HPLC chromatography. Filament assembly assays were performed as above with the addition of 25% DMSO to the buffer to prevent precipitation of the peptide. Addition of DMSO at this concentration had no effect on filament assembly.

Analytical Ultracentrifugation

All analytical ultracentrifugation samples were extensively dialyzed into a moderate-salt phosphate buffer (10mM KPO_4, pH 7.5; 150mM KCl; 5mM $MgCl_2$; 1mM EGTA; 1 mM DTT) prior to the experiment. Sedimentation velocity experiments were conducted with 10 μM protein (about 0.7 mg/mL) in a Beckman XL-1 analytical ultracentrifuge in a two-channel ultracentrifuge cell with sapphire windows. The samples were centrifuged at 50,000 rpm at 20 ˚C for 8 h, and interference scans were collected every three minutes. The data were subjected to analysis using Sedfit (P. Schuck, National Institutes of Health (Schuck, 2004)). Fits were considered satisfactory if the root-mean-squared

deviation was less than 0.01 and the residuals were random and constituted less than 10% of the original signal.

Cell Culture, RNAi, and Immunostaining

All transfectants were cloned into a pMT vector modified to express an NH_2-terminal GFP tag using EcoRI and NotI restriction sites. *Drosophila* Schneider (S2) cells were maintained in Schneider's medium with 10% fetal bovine serum (FBS) at room temperature. Approximately 3×10^6 cells were seeded per well in a 6-well plate and transfected with 0.8 μg total DNA per well using the Effectene transfection kit (Qiagen) as directed by the manufacturer's protocol.

RNAi primers were designed using T7 promoter tags to amplify the region of the Zip motor domain used by Uehara, *et al.* in ref. (18) as well as ~300 bp of the 5'-UTR of the Sqh mRNA. PCR was used to amplify the DNA template, and the Megascript T7 kit (Invitrogen) was used for transcription in accordance with the manufacturer's directions. Approximately 10^6 transfected S2 cells were transferred into 1 mL of serum-free Schneider's media along with the RNA. After 1h 2mL of Schneider's media with 10% FBS was added. This was incubated to 3 days before induction of expression with $CuSO_4$. Knockdown of Zip was verified by western blot of uninduced cells, while Sqh knockdown was observed phenotypically.

After 1d of expression, 150 μL of S2 cells were placed on 12-mm glass coverslips, allowed to settle for 1h, and fixed with paraformaldehyde for 10m. The slides were then washed three times in wash buffer (0.1% saponin in PBS) for

10 m each and mounted in Vectashield Hardset mounting medium (Vector Laboratories, inc.). Images were taken with a confocal microscope using an oil immersion 60× 1.4 NA objective. Raw images with low intensity were enhanced using the Photoshop levels command to increase pixel intensity range, and the entire panel was subjected to uniform image processing.

CHAPTER III

IDENTIFYING FLEXIBLE HINGES IN THE TAIL DOMAIN OF NON-MUSCLE MYOSIN II

The experiments described in this chapter were designed together with Dr. Kenneth E. Prehoda.

Introduction

Non-muscle myosin II (NM-II) is an actin motor protein that has three primary domains: a motor domain head, a short neck domain, and a long coiled-coil tail that is over 100 residues in length. The heavy chain is typically a dimer, with the dimerization being mediated by the coiled coil in the tail domain. The tail domain also mediates the formation of higher-order bipolar filaments. These filaments are essential for the production of contractile forces in the cell and is regulated by phosphorylation of the regulatory light chain (RLC).

RLC phosphorylation regulates motor domain activity, filament assembly, and a large conformational shift (Adelstein and Conti, 1975; Trybus and Lowey, 1984; Citi et al., 1987). When the RLC is unphosphorylated the tail forms an autoinhibited state, which is characterized by folding back of the coiled-coil tail domain. RLC phosphorylation also regulates the enzymatic activity of the motor domain, although these two events are not directly coupled (Trybus et al., 1997).

Coiled coils are one of the most commonly occurring protein structural motifs. The primary characteristic of all coiled coils is a 7-residue heptad repeat with hydrophobic residues at every first and fourth residue (fig. 1A). These hydrophobic residues allow the two α-helices to form complementary hydrophobic faces, which come together to form the core of the coiled coil (Parry et al., 2008). These interactions can be augmented by complementarity between the residues that flank the hydrophobic core. When flanking residues of opposite charge are able to interact, they can strengthen the coiled coil. On the other hand, if non-hydrophobic residues are substituted into core positions or residues of like charge are put into flanking positions, it can potentially weaken the coiled coil. The typical roles of coiled coils is to dimerize proteins and to create stiff, extended structures. A typical coiled coil has a persistence length between 25 and 150 nm (Wolgemuth and Sun, 2006). However, in inactive NM-II, the coiled coil forms tight bends and folds back on itself .

It has long been assumed that the hinges in myosin II result from regions of the coiled coil that are weaker than the idealized coiled coil. The first attempts to find the position of the flexible hinge regions of myosin II used analysis of the coiled-coil sequence to find “skip residues” where the heptad repeat was disrupted (Offer, 1990). This suggested three positions where the coiled coil should be weaker. More recently, chemical cross-linking and cryo-EM imaging of the tail have been used to ascertain the location of the tail bends (Burgess et al., 2007). While these studies have located prospective regions, they have given conflicting results as to the exact location of the bends in the tail. None of these studies have addressed the question of whether the hinge was formed by a tight

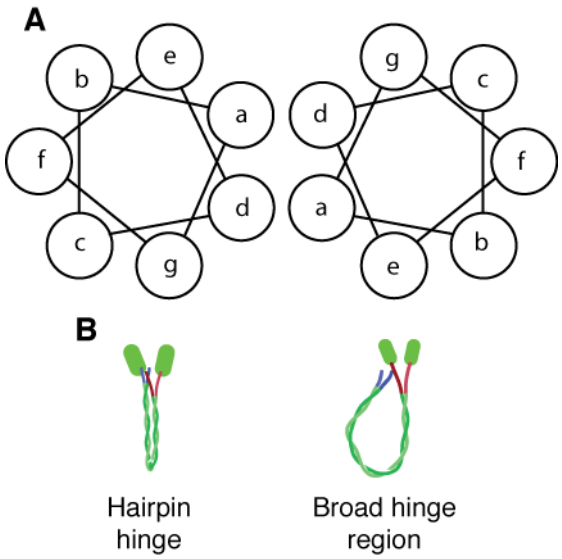

Figure 1. Bending models of the coiled coil tail of NM-II. (A) Schematic showing the layout of the positions in the coiled-coil heptad repeat. (B) Models showing the two possible types of bends in the coiled-coil tail of NM-II: the tight hairpin skip residue hinge and the broad flexible region hinge.

hairpin bend, or whether the hinge is formed by a broader bend of an entire weakened region of the coiled coil (fig. 1B).

In this study we have taken a biochemical and biophysical approach to the question of hinge location and coiled-coil stability. An analysis of the biochemical properties of the coiled coil will allow for a more definitive statement of the location and properties of the hinge domain. Thus, we have used thermal stability assays and filament assembly assays to locate the flexible hinge regions.

Results

Deleting Small Segments of an Autoinhibited Tail Fragment Restores Filament Assembly by Removing a Flexible Hinge

The flexible regions of the NM-II tail, which allow folding back of the tail and autoinhibition, have previously been studied primarily by sequence analysis (Offer, 1990), analysis of electron micrographs, and inferences from cross-linking assays. In this paper we have used biochemical assays to specify which of these elements are necessary for tail folding. In Chapter II of this Dissertation we demonstrated that a C-terminal region of the tail, when fused to the neck domain, is autoinhibited for filament assembly. This autoinhibition is accompanied by a shift to a more compact conformation, as is the case with the full-length tail, although the shift is smaller in magnitude. In this minimal system, we sought to identify the elements that allow it the in trans interactions that allow the autoinhibition to occur.

We first attempted to identify the region of the hinge using deletions. Since the autoinhibition of this region is length-dependent, we added an

additional 28 residues of the coiled coil to the N-terminus, and deleted 28-residue regions within the coiled coil. We used multiples of 7 to avoid disrupting the heptad repeat of the coiled coil, and thus introducing potential novel flexible regions. These deletions are illustrated in figure 2A. As shown in figure 2B we found that deleting the regions 1737-1764 and 1765-1792 resulted in a restoration of filament assembly. This led us to suspect that the hinge that allows autoinhibitory interactions to take place is within this region.

Changing the Protein Sequence to Mimic a Canonical Coiled Coil Stiffens and Stabilizes the Hinge

To further specify the region responsible for allowing flexibility, we created versions of our autoinhibited fragment with small sets of point mutations. These mutations were chosen to "correct" skip residues and other deviations from the canonical heptad repeat in the tail. If the hinge was a result of weakness in the coiled coil, we expected these mutations to stabilize and stiffen the coiled coil. These point mutations are outlined in figure 2C. We the performed filament assembly assays of these mutants, the results of which are shown in figure 2D, showed that several of the stabilized mutants were able to increase the proportion of filaments in the assay, indicating the these mutants were indeed rescuing the filament assembly of an autoinhibited fragment.

In order to determine the role of thermodynamic stability of the coiled coil, we put these same mutations into a short context, subcloned, and expressed the hinge domain with the various mutations that we had proposed to increase the hinge's coiled-coil stability. Within this domain we made several types of point

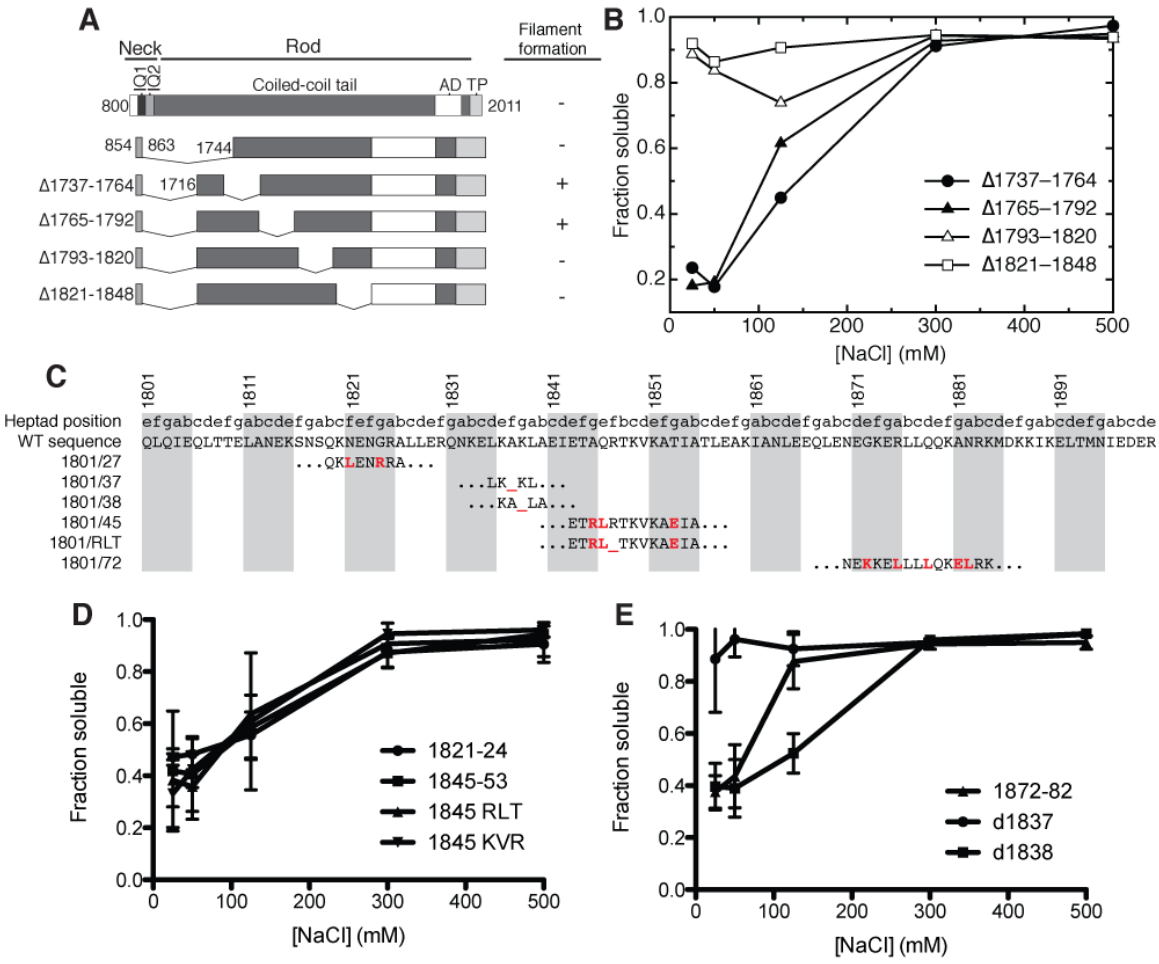

Figure 2. Locating carboxy-terminal hinge region of the NM-II coiled-coil tail. (A) A schematic illustrating the minimal autoinhibited fragment of NM-II and the deletions that were made inside of it to determine the location of the flexible hinge region. (B) Salt-dependent pelleting assays demonstrate that deletions of A.A.1737-1764 or A.A. 1765-1792 restores filament assembly to an autoinhibited fragment, while deletions of other regions does not. (C) Alignment showing the sets of point mutations or point deletions that were tested for the ability to rescue filament assembly. (D-E) Salt-dependent pelleting assays of the autoinhibited fragment with the indicated mutations. All of the mutations except d1837 had a small rescuing effect on filament assembly, although none restored filament assembly to the level of A.A. 1744-2011 without the fused IQ motif.

mutations aimed at stabilizing the coiled coil by making the sequence more similar to the idealized heptad repeat. We then melted these mutated hinge domains while observing their structural changes by circular dichroism, as shown in figure 2E. We found that the mutations at A.A. 1837 and A.A. 1872 had the most significant increases in the melting point, as compared to the wild-type sequence.

Predicted Low-Probability Coiled-Coil Regions Correlate with Low-Stability Tail Regions

Several algorithms have been designed to identify regions of proteins likely to form coiled coils. We have used the COILS algorithm (Lupas et al., 1991) to analyze the coiled-coil rod of NM-II. The result of this analysis is shown in figure 3A. Several regions with reduced coiled-coil probability are shown, including three particularly low-probability regions. Analysis electron micrographs of the NM-II hinge region have shown the presence of two bends (Onishi et al., 1983; Liu et al., 2003), which correspond with the weakened regions near AA 1200 and AA 1500. Protein sequence analysis has suggested that skip residues may have an impact on the stability. In addition to the putative hinges, there is also a particularly weak spot near the assembly domain near the C-terminus.

In order to experimentally verify these weakened sequences, we made short (100-residue) fragments of the coiled coil tail. We then used thermal melting observed by changes in the circular dichroism to quantify the thermal stability of these fragments. The results of these experiments are shown in figure 3B-D. There is a wide range of stabilities among these fragments. The N-terminal

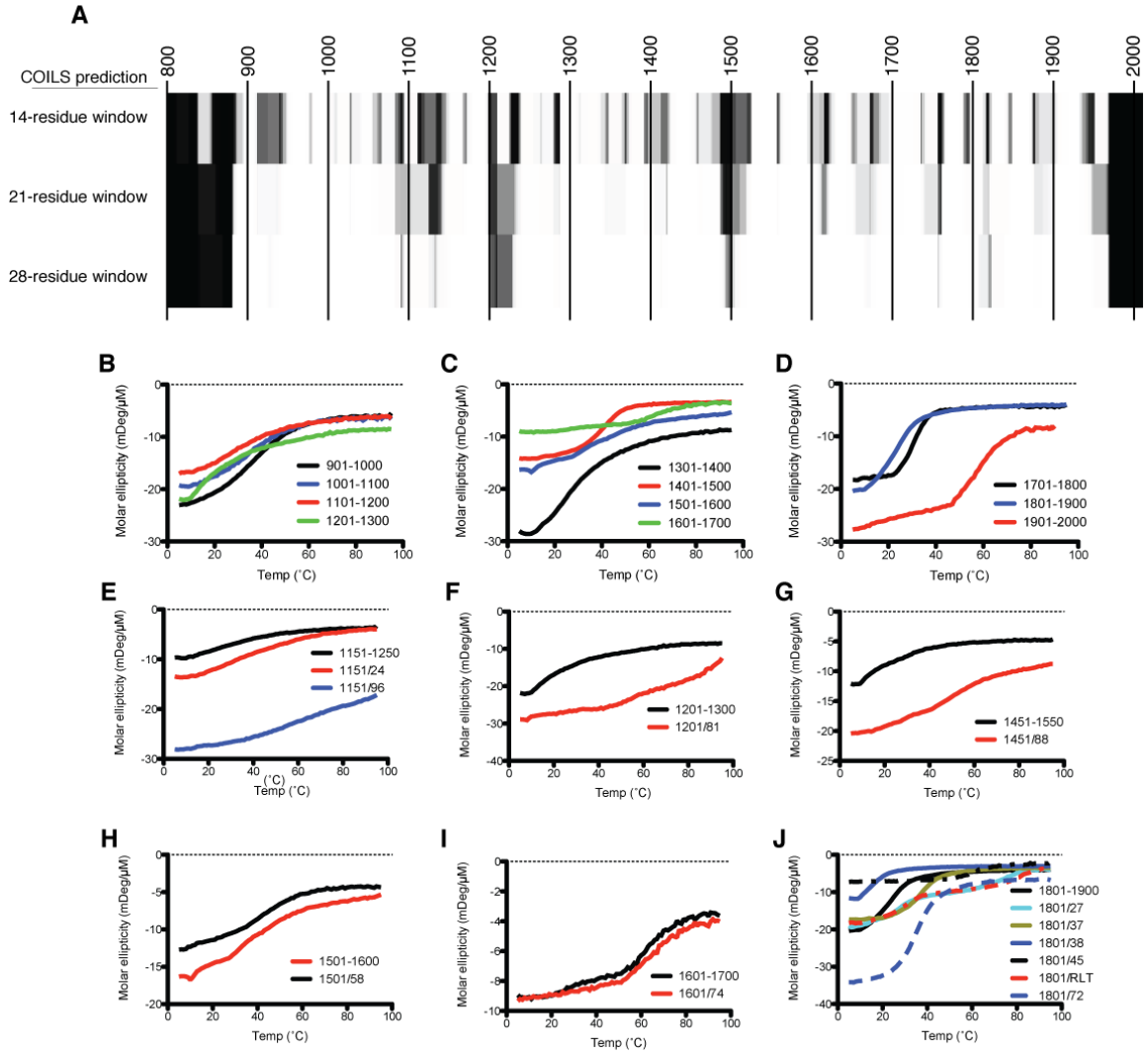

Figure 3. Coiled coil probability prediction and stability measurements in the tail of NM-II. (A) Heatmap of the COILS coiled coil prediction leve within the NM-II coiled coil tail. Darker areas are less probable, while lighter areas are more likely to form coiled coils. The three rows are variations of the window size used by the algorithm for prediction. (B-D) Thermal stability of 100-residue fragments of the tail as measured by circular dichroism at 225 nm. (E-J) Thermal stability of point mutations that cause the sequence to mimic a more ideal coiled coil in context of 100-residue fragments. Several of these point mutations are able to stabilize regions of low coiled coil stability.

region of the coiled coil is one of the least stable regions, which is compatible with previous observations that the coiled coil in this region may dynamically fold and melt to allow the motor domains to attach to actin filaments (Li et al., 2003). Outside of the N-terminus, the other weakest regions are AA 1201-1300 and 1801-1900. The region AA 1501-1600 seemed to have a relatively high stability. We hypothesized that this may be due to the hinge falling near the boundary between two fragments, and when we tested the stability of AA 1451-1550, we found that fragment's stability to be greatly reduced. There was a similar effect near AA 1200, where the fragment 1151-1250 had a somewhat lowered thermal stability, although less pronounced.

These less-stable regions not only correlate with the predictions made by the algorithms, but also with electron microscopy. This lends support to the idea that the hinges are composed of regions of the coiled coil that have a lowered stability, and can melt when subjected to bending forces.

Point Mutations in the Rod Stabilize Weak Regions

Our next task was to verify that the less stable regions identified in the previous section were necessary to form the autoinhibited conformation. We did this by analyzing the sequence and finding the residues most likely to have a destabilizing effect in the regions we discovered. These residues included polar or charged residues in the hydrophobic core of the coiled coil and similarly charged residues flanking the core residues that might have a destabilizing effect. Then we made sets of 4 or 5 point mutations in each region that would make the local sequence conform to the canonical coiled-coil heptad repeat. We the placed

these mutations into the 100-residue contexts that we had previously used to analyzed the stability. Performing thermal melts of these regions revealed that some of the point mutations had a significant stabilizing effect on the local coiled coil, while the effect of others was insignificant.

Discussion

Prior to this Study, several analyses have been undertaken to understand how the NM-II hinge functions. Some of this work has relied on analysis of the coiled-coil rod sequence and the presence of skip residues that break the coiled coil's heptad repeat (Offer, 1990). There are several examples of this throughout the rod, including one within the minimal autoinhibited fragment (A.A. 1837). Other studies have used methods such as photo-cross linking and analysis of cryo-electron microscopy to determine the locations of the hinges (Olney et al., 1996; Salzameda et al., 2006; Burgess et al., 2007; Jung et al., 2008). These studies have succeeded in roughly mapping out the positions of the hinges. They have also suggested that these hinges play an essential role in the autoinhibition and regulation of NM-II.

Even with all of this work focused on the NM-II hinges, several fundamental questions have remained unanswered. First, the position of the hinges at the sequence level remains unknown. Because of this several theories remain as to the precise function of the hinges. A tight hairpin bend in the tail could result from the flexibility of a skip residue. Alternatively, a broader flexible region could allow for looser, more flexible bends in the rod. It has also never been tested experimentally whether the hinges are truly necessary for

autoinhibition, although this seems like a strong implication of the conformation of autoinhibited NM-II.

In this Study we have taken a biophysical approach to these questions. We used a broad analysis of the entire coiled-coil rod region to determine the relative stability throughout the rod. Our measurements indicate that there are wide variations within the coiled-coil rod. Some of these correlate with previously known unstable regions, such as the N-terminal ~200 residues. We have demonstrated that this thermal stability correlates well with the probabilities given by the COILS coiled-coil prediction algorithm. That stability would correlate with a formation predictor that uses homology to known coiled coils is somewhat surprising, but seems strongly supported by our data.

Coiled-Coil Instability Allows Relatively Unstable Regions to Form Flexible Hinges

In our analysis, we were able to isolate small sets of mutations that allow the flexibility of the hinges. We first found them by making short deletions within a minimal autoinhibited fragments. Certain deletions were able to restore filament assembly, while others did not. Making point mutations to these regions allowed us to find the small sets of residues that stiffened this hinge region. None of the point mutants that we tried had a complete effect, suggesting that it required a combination of coiled-coil weak points to have sufficient flexibility for autoinhibition. Instead of the model where single skip residues result in flexible hinges, this supports the idea that the hinges are much broader sections of unstable coiled coil. Some have suggested that interactions between sections of

the rod might help stabilize the autoinhibited 10S conformation, but long flexible regions make this less likely that it would be with “skip residue” hinges.

Varying thermal stability of the coiled coil throughout the rod domain points to the conclusion that the hinges are made flexible by means of reducing the energetic cost of unfolding the coiled coil. We saw a wide range of stabilities along the coiled-coil rod domain, and the lowest stabilities correlated quite strongly with the expected hinge positions. We also saw significantly lower stability in the N-terminal 200 residues of the coiled coil, corresponding with the unstable region identified by Li and coworkers (Li et al., 2003). In the N-terminus, this instability is thought to allow flexibility in the positioning of the motor domains along actin filaments. In this case, it would allow the coiled coil to relax and partially unfold in the presence of bending stresses, and then resuming its ordered conformation in the absences of these forces.

Conclusion

We have undertaken in this study to perform a complete biochemical analysis of the NM-II coiled coil rod. By measuring the thermal stability of short segments of that rod, we have identified the unstable regions that act as the flexible hinges. We have also revealed the fact that the NM-II coiled coil is not a homogenous, rigid rod with several essential skip residues that allow bending. It has been known for some time that there are significant variations in charge along the rod. More recently it has come to light that there is variation in the stability, particularly in the N-terminal region (Li et al., 2003) and at the C-terminus in the presence of S100A4 (Kiss et al., 2012). We have now uncovered

several other unstable regions that serve the purpose of allowing dynamic relaxation of the coiled coil structure. As we discover more details about the NM-II coiled coil rod, what began as a simple structural element that allowed multimerization into filaments is being shown to possess a variety of surprising characteristics.

Materials and Methods

Cloning, Over-Expression, and Purification

All of the NM-II fragments were sub-cloned from a plasmid containing full-length Zipper isoform B as previously described (Liu et al., 2008; Ricketson et al., 2010). We created the clones for deletional analysis by overlap extension PCR. All clones were verified by DNA sequencing. Proteins were expressed from the pET-19b derivative pBH vector (Peterson et al., 2004) in *E. coli*, and the proteins were then purified using Ni-NTA resin (Qiagen) using the manufacturer's protocol. In cases where this purification failed to yield >90% pure protein as assessed by SDS-PAGE, the proteins were further purified by ion-exchange chromatography. Purified proteins were dialyzed to a salt-free Tris buffer (20 mM Tris, pH 8.0; 1 mM EDTA; 1 mM DTT) at 4˚ C.

Filament Assembly Assay

The filament assembly assay has been described previously (Liu et al., 2008). Briefly, proteins (at 10 μM unless otherwise noted) were incubated in assembly buffer (20 mM Tris, pH 8.0; 1 mM EDTA; 1 mM DTT) with the appropriate salt concentration at 4˚ C for 30 minutes followed by

ultracentrifugation at 100,000g for 30 min. We then loaded equal volumes of the supernatant and solubilized pellet fractions onto an SDS-PAGE gel for analysis, followed by staining with Coomassie Brilliant Blue. Gels were scanned and the relative amounts in each fraction were quantified with ImageJ (NIH).

Thermal Melting Assay

CD spectra were measured using a JASCO J-720 CD spectrometer equipped with a temperature-controlling sample holder. Melting spectra were measured at 225 nm with a temperature ramp rate of 1˚C/min.

CHAPTER IV

CONCLUDING REMARKS

In the work described in this Dissertation we have investigated the elements of non-muscle myosin II (NM-II) that are involved in the formation and regulation of NM-II filament assembly and the formation of the autoinhibited 10S conformation. In particular, we have identified three components that are required for this conformation to occur. These elements are the IQ motifs in the neck domain, the carboxyl-terminal, non-coiled coil tailpiece, and the flexible hinge regions in the coiled-coil rod.

We first discovered that the light chains of the neck domain are not required to inhibit filament assembly. However, the IQ motifs that the light chains bind are required, and in fact strongly repress filament assembly on their own. This inhibition could be involved in the normal regulation of NM-II, which is instigated by RLC phosphorylation. This regulation could proceed by the RLC phosphorylation exposing the IQ motif, or by the folding-back of the motor domains exposing the IQ motif. Further experimentation is needed to test whether either of these regulatory models is accurate, or indeed whether the IQ motifs are used in the regulatory pathway at all. Another possibility is that this autoinhibition is in place to prevent the assembly of unregulated or improperly folded NM-II into active filaments, thereby reducing their effectiveness.

Another more surprising element that we found to be essential for filament assembly autoinhibition is the carboxyl-terminal tailpiece. This tailpiece is a short, non-coiled coil section that occurs downstream of the coiled-coil rod. Previous work has suggested that the tailpiece may affect the stability and structure of the bipolar filaments (Murakami et al., 1995, 1998; Even-Faitelson and Ravid, 2006; Sandquist and Means, 2008). However, this is the first suggestion that the region might play a role in autoinhibition. This model would fit with the observation that the tailpiece affects the equilibrium of bipolar filaments, since changing the ratio of autoinhibited dimers to those available for filament assembly would change the overall balance between dimers and assembled filaments. As with the RLC regulation, this effect could potentially be one that only affects heavy chain that is not bound to light chains. We have not been able to identify the interactions that the tailpiece makes that inhibit filament assembly, but such interactions could only be taking place either between the IQ motifs of the neck or a region of the coiled-coil rod that is in the last 250 residues of the tail.

The last essential element that we have investigated in this Work is the flexible hinges within the coiled-coil rod. Previous models have expected that the hinges would occur at the sites of "skip" residues that disrupt the repeat pattern of the coiled coil (Offer, 1990; Straussman et al., 2005). Recent analysis by Burgess, *et al.* (Burgess et al., 2007; Jung et al., 2008), suggested that this might not be the case, and we have found that this in fact is not adequate to describe behavior of the hinges. By analyzing the coiled coil stability along the tail, we were able to find regions of low stability separate from the previously identified

skip residues, and by stabilizing the coiled coil in these regions we established which of the putative hinges were actually used in the NM-II autoinhibited conformation.

In recent years the model of NM-II regulation has become increasingly complex. A wide range of mutations has been identified that have some effect on the filament assembly or regulation of NM-II (Murakami et al., 1998; Yamashita et al., 2000; Straussman et al., 2001; Franke et al., 2005; Ludowyke et al., 2006; Clark et al., 2008; Vicente-Manzanares et al., 2009), and it has been difficult to parse the implications of many of these mutations. They have painted a picture of the NM-II coiled coil as having much more complexity than a simple stiff rod with a limited number of single-residue hinges. As I have demonstrated, the neck, tailpiece, and hinge regions all play some important roles in regulating NM-II activity. The key to our discovery has been focusing on filament assembly separately from enzymatic activity. Arguably, filament assembly is equally important for the overall function of myosin II, yet the majority of structural studies have focused exclusively on regulation of the activity of the motor domains.

The increased understanding of the essential regulatory elements that my studies have provided will allow a framework to be built that will enable interpretation of the varied work that has been done on the NM-II neck and tail. An example of this is the complicated pathway that localizes NM-II to the cleavage furrow. Without a complete understanding of the regulation and inhibition of NM-II, it is difficult to understand the mechanisms of the various modifications and binding partners that lead to proper localization and activation.

Additionally, a complete understanding of these mechanisms will contribute to a thorough understanding of motility, adhesion, and other pathways that involve NM-II.

Several important questions have been left by this work for future consideration. One of the most conspicuous is the role of the regulatory light chain (RLC) in triggering the regulation. It is clear that the RLC can regulate the enzymatic activity of the motor domains even without the tail, but how does that regulation relate to regulation of filament assembly? How does the RLC change to make the interactions that occur for autoinhibition more favorable? And how does phosphorylation at other sites on the RLC affect the its regulatory capability? Beyond RLC regulation there are a number of other potential regulators whose effects are not understood. These include post-translational modifications on the NM-II heavy chain and binding by a number of different proteins. By understanding the means of the conformational shift and regulation, a rationale can be formed for the effects that each of these have on localization and activity.

My investigation of NM-II is a small element of a growing trend in biology. In this age of large data collection projects it has become increasingly clear that in order to develop a rational understanding of biology as a whole, the massive amounts of data collected in those endeavors need to be translated from sequences to structures, from structures to functions, from functions to systems, and from systems to organisms. In elucidating the mechanism of NM-II regulation, we are attempting to put together the pieces that explain the functions

of one essential protein, which can act as a building block to assist in understanding the broader systems at work.

REFERENCES CITED

Adelstein, R.S., and Conti, M.A. (1975). Phosphorylation of platelet myosin increases actin-activated myosin ATPase activity. Nature 256, 597–598.

Bennett, P.M. (1981). The structure of spindle-shaped paracrystals of light meromyosin. J. Mol. Biol. 146, 201–221.

Berg, R. Van Den, and Hoogenraad, C.C. (2012). Molecular motors in cargo trafficking and synapse assembly. In Synaptic Plasticity, M.R. Kreutz, and C. Sala, eds. (Vienna: Springer Vienna), pp. 173–196.

Breckenridge, M.T., Dulyaninova, N.G., and Egelhoff, T.T. (2009). Multiple regulatory steps control mammalian nonmuscle myosin II assembly in live cells. Mol. Biol. Cell 20, 338–347.

Burgess, S.A., Walker, M.L., Thirumurugan, K., Trinick, J., and Knight, P.J. (2004). Use of negative stain and single-particle image processing to explore dynamic properties of flexible macromolecules. J. Struct. Bio. 147, 247–258.

Burgess, S.A., Yu, S., Walker, M.L., Hawkins, R.J., Chalovich, J.M., and Knight, P.J. (2007). Structures of smooth muscle myosin and heavy meromyosin in the folded, shutdown state. J. Mol. Biol. 372, 1165–1178.

Cheney, R.E., and Mooseker, M.S. (1992). Unconventional myosins. Curr. Opin. Cell Biol. 4, 27–35.

Chowrashi, P.K., and Pepe, F.A. (1977). Light meromyosin paracrystal formation. J. Cell Biol. 74, 136–152.

Citi, S., and Kendrick-Jones, J. (1987). Regulation of non-muscle myosin structure and function. BioEssays 7, 155–159.

Citi, S., Smith, R.C., and Kendrick-Jones, J. (1987). Effects of light chain phosphorylation and skeletal myosin on the stability of non-muscle myosin filaments. J Mol Biol 198, 253–262.

Clark, K., Middelbeek, J., Lasonder, E., Dulyaninova, N.G., Morrice, N.A., Ryazanov, A.G., Bresnick, A.R., Figdor, C.G., and van Leeuwen, F.N. (2008). TRPM7 regulates myosin IIA filament stability and protein localization by heavy chain phosphorylation. J. Mol. Biol. 378, 790–803.

Conti, M.A., Sellers, J.R., Adelstein, R.S., and Elzinga, M. (1991). Identification of the serine residue phosphorylated by protein kinase C in vertebrate nonmuscle myosin heavy chains. Biochem. 30, 966–970.

Craig, R., Smith, R., and Kendrick-Jones, J. (1983). Light-chain phosphorylation controls the conformation of vertebrate non-muscle and smooth muscle myosin molecules. Nature 302, 436–439.

Craig, R., and Woodhead, J.L. (2006). Structure and function of myosin filaments. Curr. Opin. Struct. Biol. 16, 204–212.

Cross, R.A. (1988). What is 10S myosin for? J. Musc. Res. Cell Mot. 9, 108–110.

Dai, J., Ting-Beall, H.P., Hochmuth, R.M., Sheetz, M.P., and Titus, M.A. (1999). Myosin I contributes to the generation of resting cortical tension. Biophys. J. 77, 1168–1176.

Dantzig, J. a, Liu, T.Y., and Goldman, Y.E. (2006). Functional studies of individual myosin molecules. Annals N. Y. Acad. Sci. 1080, 1–18.

Dean, S.O., and Spudich, J.A. (2006). Rho kinase's role in myosin recruitment to the equatorial cortex of mitotic Drosophila S2 cells is for myosin regulatory light chain phosphorylation. PLoS One 1, e131.

Dominguez, R., Freyzon, Y., Trybus, K.M., and Cohen, C. (1998). Crystal structure of a vertebrate smooth muscle myosin motor domain and its complex with the essential light chain: visualization of the pre-power stroke state. Cell 94, 559–571.

Dulyaninova, N.G., Malashkevich, V.N., Almo, S.C., and Bresnick, A.R. (2005). Regulation of myosin-IIA assembly and Mts1 binding by heavy chain phosphorylation. Biochem. 44, 6867–6876.

Dunn, A.R., Chuan, P., Bryant, Z., and Spudich, J.A. (2010). Contribution of the myosin VI tail domain to processive stepping and intramolecular tension sensing. Proc. Natl. Acad. Sci. 107, 7746–7750.

Edwards, K.A., and Kiehart, D.P. (1996). Drosophila nonmuscle myosin II has multiple essential roles in imaginal disc and egg chamber morphogenesis. Development 122, 1499–1511.

Elber, R., and West, A. (2010). Atomically detailed simulation of the recovery stroke in myosin by Milestoning. Proc. Natl. Acad. Sci. 107, 5001–5005.

Even-Faitelson, L., and Ravid, S. (2006). PAK1 and aPKC regulate myosin II-B phosphorylation: a novel signaling pathway regulating filament assembly. Mol. Biol. Cell 17, 2869–2881.

Fischer, R.S., Gardel, M., Ma, X., Adelstein, R.S., and Waterman, C.M. (2009). Local cortical tension by myosin II guides 3D endothelial cell branching. Curr. Biol. 19, 260–265.

Franke, J.D., Dong, F., Rickoll, W.L., Kelley, M.J., and Kiehart, D.P. (2005). Rod mutations associated with MYH9-related disorders disrupt nonmuscle myosin-IIA assembly. Blood 105, 161–169.

Garrett, S.C., Varney, K.M., Weber, D.J., and Bresnick, A.R. (2006). S100A4, a mediator of metastasis. J. Biol. Chem. 281, 677–680.

Geeves, M.A., and Holmes, K.C. (1999). Structural mechanism of muscle contraction. Annu. Rev. Biochem. 68, 687–728.

Gennerich, A., and Vale, R.D. (2009). Walking the walk: how kinesin and dynein coordinate their steps. Curr. Opin. Cell Biol. 21, 59–67.

Hodge, T.P., Cross, R., and Kendrick-Jones, J. (1992). Role of the COOH-terminal nonhelical tailpiece in the assembly of a vertebrate nonmuscle myosin rod. J. Cell Biol. 118, 1085–1095.

Horowitz, J.A., and Hammer, J.A. (1990). A new Acanthamoeba myosin heavy chain. Cloning of the gene and immunological identification of the polypeptide. J. Biol. Chem. 265, 20646–20652.

Hostetter, D., Rice, S., Dean, S., Altman, D., McMahon, P.M., Sutton, S., Tripathy, A., and Spudich, J.A. (2004). Dictyostelium myosin bipolar thick filament formation: importance of charge and specific domains of the myosin rod. PLoS Biology 2, 1880–1892.

Houdusse, A., Kalabokis, V.N., Himmel, D., Szent-Gyorgyi, A.G., Cohen, C., and Szent-Györgyi, A.G. (1999). Atomic structure of scallop myosin subfragment S1 complexed with MgADP: a novel conformation of the myosin head. Cell 97, 459–470.

Houdusse, A., Silver, M., and Cohen, C. (1996). A model of Ca(2+)-free calmodulin binding to unconventional myosins reveals how calmodulin acts as a regulatory switch. Structure 4, 1475–1490.

Ikebe, M. (2008). Regulation of the function of mammalian myosin and its conformational change. Biochem. Bioph. Res. Co. 369, 157–164.

Ikebe, M., Ikebe, R., Kamisoyama, H., Reardon, S., Schwonek, J.P., Sanders 2nd, C.R., Matsuura, M., Sanders 2nd, C.R., and Matsuura, M. (1994). Function of the NH2-terminal domain of the regulatory light chain on the regulation of smooth muscle myosin. J. Biol. Chem. 269, 28173–28180.

Ito, M., Nakano, T., Erddi, F., and Hartshorne, D.J. (2004). Myosin phosphatase: Structure, regulation and function. Mol. Cell Biochem. 259, 197–209.

Jung, H.S., Burgess, S.A., Billington, N., Colegrave, M., Patel, H., Chalovich, J.M., Chantler, P.D., and Knight, P.J. (2008). Conservation of the regulated structure of folded myosin 2 in species separated by at least 600 million years of independent evolution. Proc. Natl. Acad. Sci. 105, 6022–6026.

Kamisoyama, H., Araki, Y., and Ikebe, M. (1994). Mutagenesis of the phosphorylation site (serine 19) of smooth muscle myosin regulatory light chain and its effects on the properties of myosin. Biochem. 33, 840–847.

Kazmierczak, K., Xu, Y., Jones, M., Guzman, G., Hernandez, O.M., Kerrick, W.G.L., and Szczesna-Cordary, D. (2009). The role of the N-terminus of the myosin essential light chain in cardiac muscle contraction. J. Mol. Biol. 387, 706–725.

Kellerman, K.A., and Miller, K.G. (1992). An unconventional myosin heavy chain gene from Drosophila melanogaster. J. Cell Biol. 119, 823–834.

Kendrick-Jones, J., Smith, R.C., Craig, R., and Citi, S. (1987). Polymerization of vertebrate non-muscle and smooth muscle myosins. J. Mol. Biol. 198, 241–252.

Kiss, B., Duelli, A., and Radnai, L. (2012). Crystal structure of the S100A4–nonmuscle myosin IIA tail fragment complex reveals an asymmetric target binding mechanism. Proc. Natl. Acad. Sci. 109, 6048–6053.

Krendel, M., and Mooseker, M.S. (2005). Myosins: tails (and heads) of functional diversity. Physiology 20, 239–251.

Kumar, V.S., O'Neall-Hennessey, E., Reshetnikova, L., Brown, J.H., Robinson, H., Szent-Gyorgyi, A.G., and Cohen, C. (2011). Structure and function of the 10S conformation of smooth muscle myosin. Biophys. J. 101, 2185–2189.

Li, Y., Brown, J.H., Reshetnikova, L., Blazsek, A., Farkas, L., Nyitray, L., and Cohen, C. (2003). Visualization of an unstable coiled coil from the scallop myosin rod. Nature 424, 341–345.

Li, Z.H., and Bresnick, A.R. (2006). The S100A4 metastasis factor regulates cellular motility via a direct interaction with myosin-IIA. Cancer Res. 66, 5173–5180.

Liu, J., Wendt, T., Taylor, D., and Taylor, K. (2003). Refined model of the 10S conformation of smooth muscle myosin by cryo-electron microscopy 3D image reconstruction. J. Mol. Biol. 329, 963–972.

Liu, S.L., Fewkes, N., Ricketson, D., Penkert, R.R., and Prehoda, K.E. (2008). Filament-dependent and -independent localization modes of Drosophila non-muscle myosin II. J. Biol. Chem. 283, 380–387.

Lowey, S., Slayter, H.S., Weeds, A.G., and Baker, H. (1969). Substructure of the myosin molecule. I. Subfragments of myosin by enzymic degradation. J. Mol. Biol. 42, 1–29.

Ludowyke, R.I., Elgundi, Z., Kranenburg, T., Stehn, J.R., Schmitz-Peiffer, C., Hughes, W.E., and Biden, T.J. (2006). Phosphorylation of nonmuscle myosin heavy chain IIA on Ser1917 is mediated by protein kinase C beta II and coincides with the onset of stimulated degranulation of RBL-2H3 mast cells. J. Immunol. 177, 1492–1499.

Lupas, A., Van Dyke, M., and Stock, J. (1991). Predicting coiled coils from protein sequences. Science (New York, N.Y.) 252, 1162–1164.

Matsumura, F., Yamakita, Y., and Yamashiro, S. (2011). Myosin light chain kinases and phosphatase in mitosis and cytokinesis. Arch. Biochem. Biophys. 510, 76–82.

May, K.M., Watts, F.Z., Jones, N., and Hyams, J.S. (1997). Type II myosin involved in cytokinesis in the fission yeast, schizosaccharomyces pombe. Cell Motil. Cytoskeleton 38, 385–396.

Mermall, V. (1998). Unconventional myosins in cell movement, membrane traffic, and signal transduction. Science 279, 527–533.

Miki, H., Okada, Y., and Hirokawa, N. (2005). Analysis of the kinesin superfamily: insights into structure and function. Trends Cell Biol. 15, 467–476.

Milton, D.L., Schneck, A.N., Ziech, D.A., Ba, M., Facemyer, K.C., Halayko, A.J., Baker, J.E., Gerthoffer, W.T., and Cremo, C.R. (2011). Direct evidence for functional smooth muscle myosin II in the 10S self-inhibited monomeric conformation in airway smooth muscle cells. Proc. Natl. Acad. Sci. 108, 1421–1426.

Mizutani, T., Haga, H., Koyama, Y., Takahashi, M., and Kawabata, K. (2006). Diphosphorylation of the myosin regulatory light chain enhances the tension acting on stress fibers in fibroblasts. J. Cell Phys. 209, 726–731.

Moore, J.R., Krementsova, E.B., Trybus, K.M., and Warshaw, D.M. (2001). Myosin V exhibits a high duty cycle and large unitary displacement. J. Cell Biol. 155, 625–635.

Murakami, N., Chauhan, V.P., and Elzinga, M. (1998). Two nonmuscle myosin II heavy chain isoforms expressed in rabbit brains: filament forming properties, the effects of phosphorylation by protein kinase C and casein kinase II, and location of the phosphorylation sites. Biochem. 37, 1989–2003.

Murakami, N., Singh, S.S., Chauhan, V.P.S., and Elzinga, M. (1995). Phospholipid binding, phosphorylation by protein kinase c, and filament assembly of the COOH-terminal heavy chain fragments of nonmuscle myosin i1 isoforms MIIA and MIIB. Biochem. 34, 16046–16055.

Nakasawa, T., Takahashi, M., Matsuzawa, F., Aikawa, S., Togashi, Y., Saitoh, T., Yamagishi, A., and Yazawa, M. (2005). Critical regions for assembly of vertebrate nonmuscle myosin II. Biochem. 44, 174–183.

Naqvi, N.I., Wong, K.C., Tang, X., and Balasubramanian, M.K. (2000). Type II myosin regulatory light chain relieves auto-inhibition of myosin-heavy-chain function. Nat. Cell Biol. 2, 855–858.

Nelson, W.D., Blakely, S.E., Nesmelov, Y.E., and Thomas, D.D. (2005). Site-directed spin labeling reveals a conformational switch in the phosphorylation domain of smooth muscle myosin. Proc. Natl. Acad. Sci. 102, 4000–4005.

Niederman, R., and Pollard, T.D. (1975). Human platelet myosin. II. In vitro assembly and structure of myosin filaments. J. Cell Biol. 67, 72–92.

Nishikawa, M., Sellers, J.R., Adelstein, R.S., and Hidaka, H. (1984). How many is enough? Exploring the myosin repertoire in the model eukaryote Dictyostelium discoideum. J. Biol. Chem. 259, 8808–8814.

Nishikawa, S., Homma, K., Komori, Y., Iwaki, M., Wazawa, T., Hikikoshi Iwane, A., Saito, J., Ikebe, R., Katayama, E., Yanagida, T., et al. (2002). Class VI myosin moves processively along actin filaments backward with large steps. Biochem. Bioph. Res. Co. 290, 311–317.

Numata, N., Kon, T., Shima, T., Imamula, K., Mogami, T., Ohkura, R., Sutoh, K.K., and Sutoh, K.K. (2008). Molecular mechanism of force generation by dynein, a molecular motor belonging to the AAA+ family. Biochem. Soc. Trans. 36, 131–135.

Odronitz, F., and Kollmar, M. (2007). Drawing the tree of eukaryotic life based on the analysis of 2,269 manually annotated myosins from 328 species. Gen. Biol. 8, R196.

Offer, G. (1990). Skip residues correlate with bends in the myosin tail. J. Mol. Biol. 216, 213–218.

Olney, J.J., Sellers, J.R., and Cremo, C.R. (1996). Structure and function of the 10S conformation of smooth muscle myosin. J. Biol. Chem. 271, 20375–20384.

Onishi, H., Wakabayashi, T., Kamata, T., and Watanabe, S. (1983). Electron microscopic studies of myosin molecules from chicken gizzard muscle II: The effect of thiophosphorylation of the 20K-dalton light chain on the ATP-induced change in the conformation of myosin monomers. J. Biochem. 94, 1147–1154.

Parry, D.A.D., Fraser, R.D.B., and Squire, J.M. (2008). Fifty years of coiled-coils and alpha-helical bundles: a close relationship between sequence and structure. J. Struct. Biol. 163, 258–269.

Peterson, F.C., Penkert, R.R., Volkman, B.F., and Prehoda, K.E. (2004). Cdc42 regulates the Par-6 PDZ domain through an allosteric CRIB-PDZ transition. Mol. Cell 13, 665–676.

Pufall, M.A., and Graves, B.J. (2002). Autoinhibitory domains: modular effectors of cellular regulation. Annu. Rev. Cell Dev. Biol. 18, 421–462.

Quevillon-Cheruel, S., Janmot, C., Nozais, M., Lompre, A.-M., and Bechet, J.-J. (2000). Functional regions in the essential light chain of smooth muscle myosin as revealed by the mutagenesis approach. Eur. J. Biochem. 267, 6151–6157.

Rayment, I., Holden, H.M., Whittaker, M., Yohn, C.B., Lorenz, M., Holmes, K.C., and Milligan, R.A. (1993a). Structure of the actin-myosin complex and its implications for muscle contraction. Science 261, 58–65.

Rayment, I., Rypniewski, W.R., Schmidt-Bäse, K., Smith, R., Tomchick, D.R., Benning, M.M., Winkelmann, D.A., Wesenberg, G., and Holden, H.M. (1993b). Three-dimensional structure of myosin subfragment-1: a molecular motor. Science 261, 50–58.

Rayment, I., Smith, C., and Yount, R.G. (1996). The active site of myosin. Ann. Rev. Phys. 58, 671–702.

Richards, T.A., and Cavalier-Smith, T. (2005). Myosin domain evolution and the primary divergence of eukaryotes. Nature 436, 1113–1118.

Ricketson, D., Johnston, C.A., and Prehoda, K.E. (2010). Multiple tail domain interactions stabilize nonmuscle myosin II bipolar filaments. Proc. Natl. Acad. Sci. 107, 20964–20969.

Ronen, D., and Ravid, S. (2009). Myosin II tailpiece determines its paracrystal structure, filament assembly properties, and cellular localization. J. Biol. Chem. 284, 24948–24957.

Salzameda, B., Facemyer, K.C., Beck, B.W., and Cremo, C.R. (2006). The N-terminal lobes of both regulatory light chains interact with the tail domain in the 10S-inhibited conformation of smooth muscle myosin. J. Biol. Chem. 281, 38801–38811.

Sandquist, J.C., and Means, A.R. (2008). The C-terminal tail region of nonmuscle myosin II directs isoform-specific distribution in migrating cells. Mol. Biol. Cell 19, 5156–5167.

Schuck, P. (2004). A model for sedimentation in inhomogeneous media. I. Dynamic density gradients from sedimenting co-solutes. Biophys. Chem. 108, 187–200.

Sellers, J.R. (1999). Myosins (Oxford: Oxford University Press).

Sellers, J.R. (2000). Myosins: a diverse superfamily. Biochim. Biophys. Acta 1496, 3–22.

Sellers, J.R., and Knight, P.J. (2007). Folding and regulation in myosins II and V. J. Muscle Res. Cell Motil. 28, 363–370.

Sellers, J.R., Pato, M.D., and Adelstein, R.S. (1981). Reversible phosphorylation of smooth muscle myosin, heavy meromyosin, and platelet myosin. J. Biol. Chem. 256, 13137–13142.

Sheng, S., Gao, Y., Khromov, A.S., Somlyo, A.P.A. V, Somlyo, A.P.A. V, and Shao, Z. (2003). Cryo-atomic force microscopy of unphosphorylated and thiophosphorylated single smooth muscle myosin molecules. J. Biol. Chem. 278, 39892–39896.

Soldati, T., Geissler, H., and Schwarz, E.C. (1999). How many is enough? Exploring the myosin repertoire in the model eukaryote Dictyostelium discoideum. Cell Biochem. Biophys. 30, 389–411.

Spudich, J.A., and Sivaramakrishnan, S. (2010). Myosin VI: an innovative motor that challenged the swinging lever arm hypothesis. Nat. Rev. Mol. Cell Biol. 11, 128–137.

Straussman, R., Even, L., and Ravid, S. (2001). Myosin II heavy chain isoforms are phosphorylated in an EGF-dependent manner: involvement of protein kinase C. J. Cell Sci. 114, 2057–3047.

Straussman, R., Squire, J.M., Ben-Ya'acov, A., and Ravid, S. (2005). Skip residues and charge interactions in myosin II coiled-coils: implications for molecular packing. J. Mol. Biol. 353, 613–628.

Trybus, K.M., Freyzon, Y., Faust, L.Z., and Sweeney, H.L. (1997). Spare the rod, spoil the regulation: necessity for a myosin rod. Proc Natl Acad Sci U S A 94, 48–52.

Trybus, K.M., Huiatt, T.W., and Lowey, S. (1982). A bent monomeric conformation of myosin from smooth muscle. Proc. Natl. Acad. Sci. 79, 6151–6155.

Trybus, K.M., and Lowey, S. (1984). Conformational states of smooth muscle myosin. Effects of light chain phosphorylation and ionic strength. J. Biol. Chem. 259, 8564–8571.

Trybus, K.M., and Lowey, S. (1987). Assembly of smooth muscle myosin minifilaments: effects of phosphorylation and nucleotide binding. J. Cell Biol. 105, 3007–3019.

Tyska, M.J., and Mooseker, M.S. (2003). Myosin-V motility: these levers were made for walking. Trends Cell Biol. 13, 447–451.

Tyska, M.J., and Warshaw, D.M. (2002). The Myosin power stroke. Cell Motil. Cytoskeleton 51, 1–15.

Ueda, K., Murata-Hori, M., Tatsuka, M., and Hosoya, H. (2002). Rho-kinase contributes to diphosphorylation of myosin II regulatory light chain in nonmuscle cells. Oncogene 21, 5852–5860.

Uehara, R., Goshima, G., Mabuchi, I., Vale, R.D., Spudich, J. a, and Griffis, E.R. (2010). Determinants of myosin II cortical localization during cytokinesis. Curr. Biol. 20, 1080–1085.

Vicente-Manzanares, M., Ma, X., Adelstein, R.S., and Horwitz, A.R. (2009). Non-muscle myosin II takes centre stage in cell adhesion and migration. Nat. Rev. Mol. Cell Biol. 10, 778–790.

Wang, A., Ma, X., Conti, M.A., and Adelstein, R.S. (2011). Distinct and redundant roles of the non-muscle myosin II isoforms and functional domains. Biochem. Soc. Trans. 39, 1131–1135.

Wolgemuth, C.W., and Sun, S.X. (2006). Elasticity of alpha-helical coiled coils. Phys. Rev. Lett. 97, 248101.

Yamashiro, S., Totsukawa, G., Yamakita, Y., Sasaki, Y., Madaule, P., Ishizaki, T., Narumiya, S., and Matsumura, F. (2003). Citron kinase, a rho-dependent kinase, induces di-phosphorylation of regulatory light chain of myosin II. Mol. Biol. Cell 14, 1745–1756.

Yamashita, H., Tyska, M.J., Warshaw, D.M., Lowey, S., and Trybus, K.M. (2000). Functional consequences of mutations in the smooth muscle myosin heavy chain at sites implicated in familial hypertrophic cardiomyopathy. J. Biol. Chem. 275, 28045–28052.